TRABAJO FIN DE GRADO

Grado en Ingeniería Electrónica Industrial

UNIVERSIDAD DE ALMERIA

ESCUELA SUPERIOR DE INGENIERÍA

Development of a control system for general anesthesia

Curso 2018/2019

Alumno/a:

Paolo Visieri

Director/es:

Dr. D. Antonio Visioli

Dr. D. Andrzej Pawlowski

Resumen/Abstract

Nowadays control technologies have a great importance for modern medicine, as they influence different clinical practices. In fact, new discoveries in biology and a better understanding of the biological functions allow the development of new sensors, actuators and more accurate models of the human body response to the administration of drugs. This has led to the introduction of control systems also in drug administration contexts, among which the closed-loop control of anesthesia during surgeries is one of the most important. General anesthesia provides a suitable level of hypnosis, neuromuscular blockade and analgesia to the patient under surgery and each of these effects is regulated by using a specific drug. In order to achieve adequate levels of anesthesia, the anesthesiologists must adjust several parameters, and the choice is made relying on experience, on recommended doses, and on the trends of specific vital signs of the patient. To ease the burden of this crucial role, a solution may be given by introducing model based closed-loop control techniques. These strategies are based on the availability of a patient model and then the role of the anesthesiologist will be freed of some regular tasks so that he/she can focus more on the state of the patient. The aim of this work is to develop a model-based scheme to control the depth of hypnosis in anesthesia using the BIS signal as controlled variable. In particular, control scheme based on GPC has been firstly developed in order to regulate the infusions of the anesthetic drug Propofol. The PK-PD model of the patient is exploited so that the estimated effect-site concentration is used as a feedback signal. Then, after testing the system robustness, the obtained scheme has been expanded to control also the infusions of the analgesic drug remifentanil.

Doble TítuloUNIBS-UAL

Mechatronics for Industrial Automation

Ingegneria dell'Automazione Industriale

Grado en Ingeniería Electrónica Industrial

Curso 2018/2019

UNIVERSIDAD DE ALMERÍA
Escuela Superior de Ingeniería

UNIVERSITÀ DEGLI STUDI DI BRESCIA
Dipartimento di Ingegneria Meccanica Industriale
Corso di Laurea Magistrale in Ingegneria dell'Automazione Industriale

Trabajo Fin de Grado
Ingeniería Electrónica Industrial

Development of a control system for general anesthesia

Desarrollo de un sistema de control para anestesia general

Doble Título UNIBS-UAL
Mechatronics for Industrial Automation

Autor: Paolo Visieri

Director: Dr. D. Antonio Visioli
Codirector: Dr D. Andrzej Pawlowski

Almería (España), Diciembre 2018
Curso 2018-2019

Abstract

Nowadays control technologies have a great importance for modern medicine, as they influence different clinical practises. In fact, new discoveries in biology and a better understanding of the biological functions allow the development of new sensors, actuators and more accurate models of the human body response to the administration of drugs. This has led to the introduction of control systems also in drug administration contexts, among which the closed-loop control of anesthesia during surgeries is one of the most important. General anesthesia provides a suitable level of hypnosis, neuromuscular blockade and analgesia to the patient under surgery and each of these effects is regulated by using a specific drug. In order to achieve adequate levels of anesthesia, the anesthesiologists must adjust several parameters, and the choice is made relying on experience, on recommended doses, and on the trends of specific vital signs of the patient. To ease the burden of this crucial role, a solution may be given by introducing model based closed-loop control techniques. These strategies are based on the availability of a patient model and then the role of the anesthesiologist will be freed of some regular tasks so that he/she can focus more on the state of the patient. The aim of this work is to develop a model-based scheme to control the Depth of Hypnosis (DoH) in anesthesia using the Bispectral Index Scale (BIS) signal as controlled variable. In particular, control scheme based on Generalized Predictive Control (GPC) will be firstly developed in order to regulate the infusions of the anesthetic drug propofol, exploiting the PKPD model of the patient so that the estimated effect-site concentration is used as a feedback signal. Then, the obtained scheme will be expanded to control also the infusions of the analgesic drug remifentanil.

Contents

List of Figures

List of Tables

List of Acronyms

BIS Bispectral Index Scale

CARMA Controller Auto-Regressive Moving-Average

DoH Depth of Hypnosis

EEG Electroencephalogram

GA Genetic Algorithms

GPC Generalized Predictive Control

IAE Integral Absolute Error

IMC Internal Model Control

LTI Linear Time Invariant

MCM Monte Carlo Method

MISO Multiple Input Single Output

mp-MPC multi-parametric MPC

MPC Model Predictive Control

NMB Neuromuscular Blockade

PD Pharmacodynamics

PID Proportional-Integrative-Derivative control law

List of Acronyms

PK Pharmacokinetics

PKPD Pharmacokinetic - Pharmacodynamic

SISO Single Input Single Output

SMMAC Supervised Multi-model Adaptive Control

TCI Target Controlled Infusion system

TIVA Total Intravenous Anesthesia

Chapter 1

Introduction

Undergoing a surgical procedure has become nowadays a rather common event in one's life, however what is behind this process is almost unknown for the majority of the people. The aim of this chapter is to introduce the reader with an overview of the concepts now in use in this medical field and the short history presented in the first section will emphasize the tremendous impact that the discovery of anesthesia had in medicine as well as the numerous developments that have taken place ever since. The concepts and definition of anesthesia, as well as the possible risks, will be presented. Then, a brief overview of the anesthesiologist's work is reported in order to highlight the advantages that a closed loop control system could bring. Finally, in the last section, the equations that make up the models will be described in detail.

Temporal organization

The Gantt diagram that shows how the work has been developed is shown in figure 1.1. The literature review phases consist in the search and assimilation of the knowledge necessary to carry out the rest of the project. There are two phases because the work is firstly focused on the control of the propofol only, SISO development phase, and then, after obtaining a good control sister, it is possible to expand it to control also the remifentanil infusions, MISO development phase. Tests were carried out for each structure, in order to

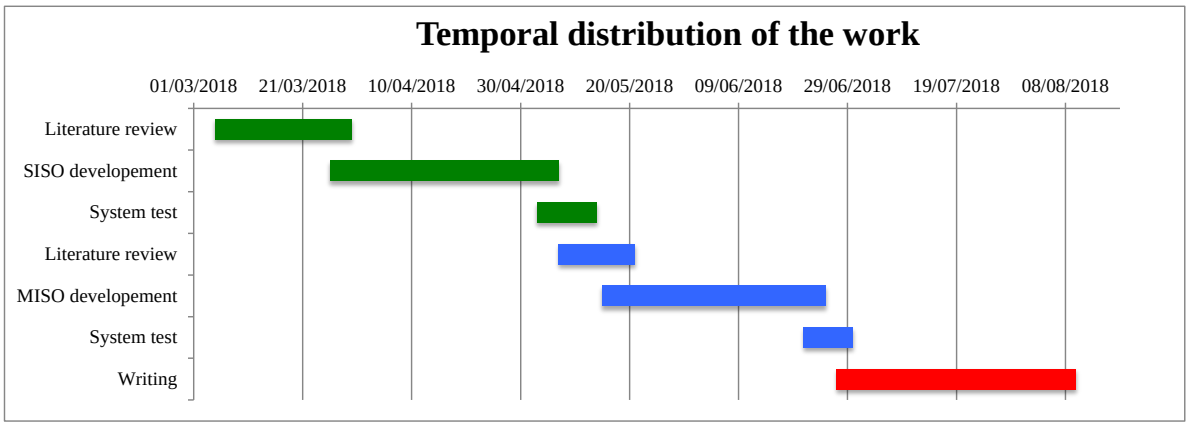

Figure 1.1: Gantt diagram with the temporal distribution.

evaluate the performance and make comparison with other works.

1.1 Clinical anesthesia

General anaesthesia is generally considered to have been born on 16$^{\text{th}}$ October 1846, when dentist William T. G. Morton demonstrated the use of ether inhalation for surgical anaesthesia on a patient at Massachusetts General Hospital. Ether anaesthesia was subsequently quickly adopted around the world, but before that day surgery was uncommon and often a horrific experience for the patient. In fact the techniques used to slightly reduce the pain, such as nerve compression or application of cold, allowed only surgical procedures with extremely fast execution. Decreased cerebral perfusion obtained by compressing the carotid artery was also used to render the patient unconscious, as well as the use of alcohol and drugs but morbidity and mortality was very high. For that reason the success of the 'etherization' procedure, as it was first called by its inventor, immediately obtain great echo throughout the civilized world. The term 'anesthesia', from the Greek word $\alpha\nu\alpha\iota\sigma\theta\eta\sigma\iota\alpha$, the lack of sensitivity, was later proposed to Morton by Oliver Wendell Holmes to describe that new phenomenon.

Since the birth of the anesthesia a lot of different anesthetic agents has been investigated, and parallel to that the 19$^{\text{th}}$ century witnessed the invention of many inhalation apparatuses

and techniques for drugs administration. The increasing complexity of the administration and management of anesthesia requested the introduction of a new role in the surgery room, and in the 1935 the first diploma of anesthesia was offered.

1.1.1 Risk and outcome in anesthesia

Development of anesthesia since the 19^{th} century was concentrated on the safety of the patient. In fact, by the end of 19^{th} century the incidence of death due to anesthesia was less than 0.1% [1]. A 1986 survey revealed that the overall death rate directly attributable to anesthetic drugs was 1:185 056. Human error is probably the most common cause of death, in fact, according to a 1987 study 75% of anesthetic related deaths are due to anesthesiologist failure to apply life-savings knowledge, while only 1.7% of cases involve equipment failure. This very low mortality rate can be attributed mainly to the following three aspects of the clinical practice:

1. First, anesthesiologist select an appropriate combination of drugs and drug dosage according the patient's age, weight, co-morbid disease and the type and duration of the operation. In standard practise the anesthesiologist often uses several drugs in order to reach a state of *balanced anesthesia*, thus limiting the potential lethal side effects of each drug.

2. The second aspect concerns the equipment that monitor patient's vital signs and eventually warns the practitioner of possible complications. Modern equipment is fairly sophisticated and includes standard devices such as mass spectrometers capnographs, pulse oximeters, heart rate and blood pressure monitors, etc.

3. Finally, education has had a key role in making anesthesia a particularly safe and reliable procedure. Postgraduate training programs in the speciality of anesthesiology are offered by every major medical school. Also this medical speciality benefits from the publication of numerous clinical research journals, such as Anestesiology, British Journal of Anaestesia, etc...

All of these aspects contribute to make clinical anesthesia one of the safest components of any surgical operation: even particularly ill patients can be safely anesthetized. It is the surgical procedure itself which offers the most risk. However, older adults and those undergoing lengthy procedures are most at risk of negative outcomes, which can include postoperative confusion, heart attack, pneumonia and stroke. A number of more serious complications are associated with general anaesthetics, but these are rare. Possible serious complications and risks include [2]:

- a serious **allergic reaction** to the anaesthetic (anaphylaxis);
- **waking up** during your operation. The continuous monitoring of the amount of anaesthetic given will help to ensure this doesn't happen;
- **death**, but this is very rare, occurring in around 1 in every 100 000 cases.

Serious problems are more likely to occur if the patient is having major or emergency surgery, if he/she has any other illnesses, he/she smokes, or he/she is overweight, but in most cases, the benefits of being pain-free during an operation outweigh the risks.

1.2 Modern concepts

Even though our understanding and methods of administering general anaesthesia have evolved over time we still do not have a definition of general anaesthesia that is commonly agreed upon. In 1987 Prys-Roberts describe the anesthesia as a state of "drug-induced unconsciousness, [where] the patient neither perceives nor recalls noxious stimuli" [3]. This definition limits the term of anesthesia to an absence of both conscious awareness and memory formation (i.e., *hypnosis* and *amnesia*). However, the role of the anesthesiologists goes beyond provoking a mere hypnotic state. They also ensure that autonomic reflexes involving the sympathetic and parasympathetic nervous system (to provide cardiorespiratory control) are not sensitive to surgical stress. This is achieved by inducing a state of *analgesia* with the administration of opioid drugs. Furthermore, intra-abdominal surgeries

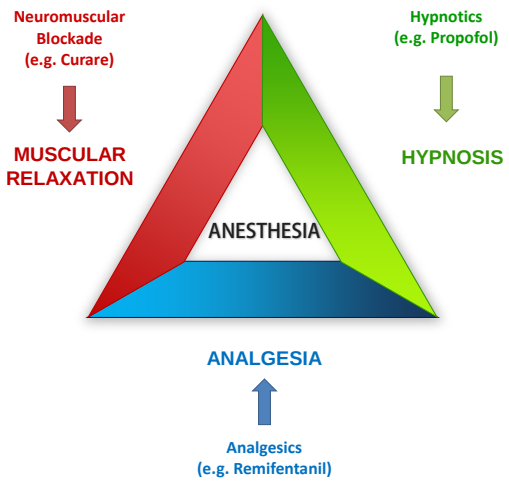

Figure 1.2: The three effects of the anesthesia.

require the blockade of reflex muscle activity in the abdominal wall in order to permit surgical exposure. To attain such state of *paralysis* it is necessary to use Neuromuscular Blockade (NMB) agents. It is important to note that these drugs act peripherally at the level of the synaptic link between the nerve and the muscle, and not centrally in the brain or the spinal cord. To summarize, it is common in the literature to consider that the state of clinical anesthesia results from the combination of three functional components, that is, hypnosis, analgesia and immobility (figure 1.2). Three broad categories of anaesthesia exist, they differentiate each other for the duration, the depth and part of the body involved:

- **General anesthesia** suppresses central nervous system activity and results in unconsciousness and total lack of sensation.
- **Sedation** suppresses the central nervous system to a lesser degree, inhibiting both anxiety and creation of long-term memories without resulting in unconsciousness.
- **Regional anesthesia** and local anesthesia, which block transmission of nerve impulses between a targeted part of the body and the central nervous system, causing loss of sensation in the targeted body part. A patient under regional or local anes-

thesia remains conscious.

There are also other type of anesthesia, used only in particulary situations, but the term *anesthesia* is usually referred to the general anesthesia. That procedure can be divided into four phases:

- The **preparation** of the patient that consist in getting the patient sedate before bringing him in the surgery room.
- The **induction** is the period between the administration of analgesic and anesthetic agents and loss of consciousness. During this stage, the patient progresses from analgesia without amnesia to analgesia with amnesia. Patients can carry on a conversation at this time
- The **maintenance** is the period in which occurs the surgical operation. During this times the drugs are dosed in order to maintain an adequate level of anesthesia.
- The **recovery** phase occurs when the drug administration ends, and the patients wakes up, recovering all of his vital functions.

The narcosis is ensured by the infusion of specific drugs, which can be administrated in two different way: by inhalation or by injection. These drugs include anesthetic to induce the unconsciousness, analgesic to reduce the pain and muscle relaxers needed to avoid involuntary movement of the patient. When necessary, other drugs can be used, for example to control the arterial pressure, the heart rate or to reduce the sickness. When the drug are administrated by intravenous route (i.e. Total Intravenous Anesthesia (TIVA)), the propofol is commonly used as anesthetic due to its hypnotic properties and the almost complete absence of side effects [4]. Propofol is generally combined with the remifentanil, a fast-acting opioid with analgesic functions [5]. When used together these drugs have a synergic effect: the remifentanil amplifies propofol's effects as well as the side effects, especially if the dosage of anesthetic is high. Hence, the study of this interaction becomes a crucial step in order to grant an adequate level of anesthesia and to regulate the correct quantity of each drug.

1.2.1 The role of the anesthesiologist

In the surgery room the management of a patient's anesthesia relies on the anesthesiologists experience and ability. The anesthesiologist has to choose the time and the sequence of the infusions, as well as the drugs dosage, based on the patient's physical characteristics, like age, height, weight, gender, physical condition, diseases and the kind of the surgery. Hence the first infusion profile is chosen on the basis of recommended doses and estimates based on mathematical models. Later, the anesthesiologist regulates the drugs dosage in function of the response to noxious stimuli and of the alterations of the hypnotic state of the patient. These alterations are determined by some indirect indicators that the anesthesiologist monitors continuously, such as heart rate, arterial pressure, electrical activity of the encephalon, tear secretion and facial contractions.

As said before, in order to blunt the effect of surgical stimulation, anesthesiologists use a combination of drugs to block sensation. However the very mechanism of action of these drugs make them particularly dangerous, as they deprive the central nervous system from the information necessary to control normal body functions (i.e., gag reflex, respiration, cardiac rhythm, and blood pressure). An overdose may then stop a patient's breathing and may even provoke a cardiovascular collapse. Overdoses are usually associated with a lack of balance between the anesthetic regimen and the patient's pharmacological needs. When there is no surgical stimulation, the patient's needs are low and a small amount of drug may be sufficient to make them comfortable. However during noxious stimuli (i.e., stimuli associated with transmission of nerve pain signals), drug titration needs to be increased to limit the effect of surgery. As a result, a common side effect is the depression of the cardiorespiratory system when surgical stimulation suddenly disappears.

Therefore, anesthesiologists try to keep a balance between the toxicity of anesthetic drugs and the noxious stimulation of surgery.

1.2.2 State of the art

Over the years a lot of indexes for the hypnotic and analgesic effects have been investigate, as well as for the muscle relaxation. NMB level is measured from the electromyography signal obtained by electrical stimulation [6]. The control of NMB is done by means of continuous infusion of a muscle relaxant and in the past years several control strategies have been developed.

As already mentioned, the typical drug used to control the DoH is propofol, due to its hypnotic properties and the almost complete lack of side effects [4]. Numerous researches have been made on the propofol using the Electroencephalogram (EEG) as measure of the anesthetic effect but the EEG cannot be used for accurate measure because of its difficult evaluation and the high content of noise that presents. For that reason preference is given to other indexes, derived from the EEG with digital signal processing, among which the most used is the BIS [7]. The BIS is widely employed to measure the level of hypnosis of the patient during anesthesia. It provides an estimation of DoH based on the bispectral analysis of the EEG resulting in a dimensionless number between 0, equivalent to EEG silence, to 100, equivalent to the patient fully awake. A target range between 40 and 60 is suggested to prevent awareness and to reduce the dose of anesthetic agent that is needed to maintain optimal anesthesia level.

The third component, the analgesia, is still to be demystified [8] and an accurate and objective measurement of the patient's response to analgesic drug is still lacking. However, when BIS is known a suitable interaction model between hypnotics and analgesics might be helpful to simultaneously control both components of depth of anesthesia [9].

In the clinical practice of TIVA, it has been demonstrated the absolute possibility of designing robust closed loop control systems even in the presence of extensive variability among patients, using, for example, combinations of robust control techniques and adaptive models [10]. The first use of computer systems in anesthesia dates back to 1996, when it was introduced the *Diprifusor* system: a software module interfaced to medical pumps which manages open-loop infusion on the basis of propofol compartment models described in the

literature [11]. This system is called Target Controlled Infusion system (TCI), and it allows a reduction of the anesthesiologist's work. In fact, with the patient's physical data and the target plasma concentration defined a priori by the doctor, the system automatically calculates the appropriate infusion rate and the anesthesiologist's task becomes that of adapting the system to the variability that is found between the different patients. This is done by adjusting the right target concentration during the surgery. Recent studies on predictive control and model-based control have allowed an improvement in stability and closed-loop performance. In literature, on the basis of Internal Model Control (IMC), robust strategies have been developed for the control of a Single Input Single Output (SISO) that uses the BIS as a control variable to automatically adjust the propofol flow exiting the pump [12]. The same type of SISO model was used both for prediction and simulation purposes. A Model Predictive Control (MPC) algorithm was then designed, showing a performance improvement over a generic predictive algorithm [13]. Studies on control systems for muscle inhibitors have been performed in [14], identifying an excellent candidate in the Supervised Multi-model Adaptive Control (SMMAC), which regulates the flow of drugs based on muscle relaxation measured by a evoked potential (EP). Subsequently, the concepts of reduced model and parameter identification were applied for the combined infusion of propofol and remifentanil using an extended Kalman filter [15].
Finally, it is right to quote other methods taking into account only propofol administration that have been proposed in the literature like [16], [17], [18] and already successfully applied in practice.

1.3 Modeling anesthetic drugs

In order to develop an automatic control system for anesthesia that satisfies the strict specifications and robustness characteristics that this problem presents, it is necessary to know the response of the human body to the infusion of drugs. Having a mathematical model that describes this behavior is therefore fundamental for carrying out simulations, verifications and validations of the designed controller. In addition to this, when predictive control is intended for a precise administration of drugs, the model used in the prediction becomes of vital importance. Such model must capture well enough the dynamics of the patient in response to the specific drugs considered. The relationship between drug infusion rate and the drug effect can be described with pharmacokinetic and pharmacodynamic models. With the Pharmacokinetics (PK) we describe the infusion, distribution and subsequent elimination of the drug in the body, indicating the plasma concentration of the medicine infused following a certain administration. With the Pharmacodynamics (PD) we describe the relationship between the plasma concentration of drugs in the blood and their clinical effect.
As already mentioned earlier, in the present thesis we refer to the use of propofol as a hypnotic drug and remifentanil as analgesic: these two drugs are characterized by a synergistic effect on the level of hypnosis of the patient: when the remifentanil is administered together with propofol, the hypnotic effect is amplified. The model, in addition to the PK and PD parts of both, must take into account also this mutual interaction and describe it appropriately.

In this work, we use the Shnider model [19] for the description of the propofol response and the Minto model [20] for remifentanil. They provide a linear dynamic part given by the pharmacokinetic and pharmacodynamic series in addition to a non-linear Hill function which represent the synergistic effect of the two drugs over the BIS. To simplify the representation and to facilitate the development of automatic control, only the SISO model describing the effect of propofol on the BIS will be initially presented, without considering the use of analgesics. Only later the problem will be extended to the use of the two drugs,

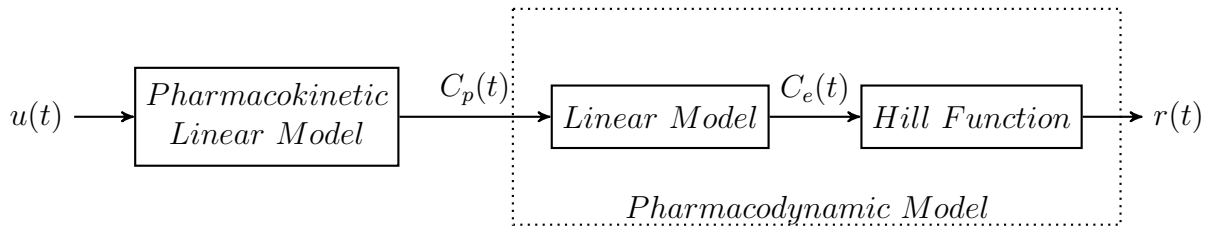

Figure 1.3: Block diagram of the propofol model including Pharmacokinetic parts and Pharmacodynamics [14]

exploiting the complete model with the two linear parts and the Hill function.

1.3.1 SISO model

Among the drugs that can guarantee patient hypnosis, propofol is certainly the most noteworthy. By studying his behavior, several models have been constructed. These models relate the infusion rate and the level of hypnosis achieved measured by the BIS index, but among them, the version universally accepted in the literature is that of Schnider [19]. Like all pharmacological models it is composed of a pharmacokinetic part followed in cascade by a pharmacodynamic part as illustrated in figure 1.3.

Pharmacokinetics of propofol

Pharmacokinetics is usually described by means of mamillary compartmental models, where it is assumed that each compartment presents homogeneous properties; in particular the instantaneous drug distribution inside a compartment is uniform. The propofol response model is made up of three compartments, as shown in figure 1.4. Each compartment represent one part of the body:

- **primary compartment**: it is identifiable with blood, as it receives directly the drug via drip.
- **fast compartment**: it interacts directly with the primary compartment. It is the logical representation of organs and muscles that interact with blood through dynamics that can be considered fast.

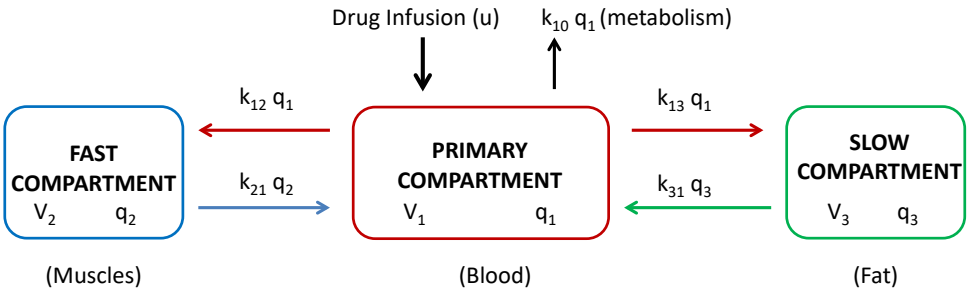

Figure 1.4: Block diagram of the Pharmacokinetics of the propofol.

- **slow compartment**: similar to the fast one, it only interacts with the primary compartment. It represents tissues that are in interchange relations with blood through slow dynamics. This category includes, for example, fatty masses.

Starting from the block diagram we can reconstruct the equations that describe the inter-compartmental bonds:

$$\begin{aligned} \dot{q}_1(t) &= -(k_{10} + k_{12} + k_{13})q_1(t) + k_{21}q_2(t) + k_{31}q_3(t) + u(t) \\ \dot{q}_2(t) &= k_{12}q_1(t) - k_{21}q_2(t) \\ \dot{q}_3(t) &= k_{13}q_1(t) - k_{31}q_3(t) \end{aligned} \tag{1.1}$$

Where:

- $u(t)$ indicates the speed of the incoming drug. This is called **mass flow**, as it represents the entering mass over the unit of time. Usually, in the surgery room, the units of measurement are $[mg/s]$ for propofol and $[\mu g/s]$ for remifentanil;
- $q_i(t)$ indicates the current mass of propofol in the ith compartment;
- $\dot{q}_i(t)$ indicates the input (if positive) or output (negative) flow of the ith compartment of the block diagram;
- k_{ij} is a parameter with dimension $[1/s]$ that models the flow of drug from the ith to jth compartment. In particular, k_{10} represents the drug eliminated through metabolic process.

As proposed by Schnider, the k_{ij} values can be calculated from the relationship between Clearance[1] (Cl_i) of the compartment of arrival and volume of the one of departure[2]:

$$\begin{aligned} k_{10} &= \frac{Cl_1}{60V_1}; \quad k_{12} = \frac{Cl_2}{60V_1}; \; k_{13} = \frac{Cl_3}{60V_1}; \\ k_{21} &= \frac{Cl_2}{60V_2}; \quad\; k_{31} = \frac{Cl_3}{60V_3}. \end{aligned} \tag{1.2}$$

The values of V_i can be calculated in $[l]$ using the following equations:

$$V_1 = 4.27, \quad V_2 = 18.9 - 0.391(Age - 53), \; V_3 = 2.38; \quad [l] \tag{1.3}$$

Where Age is dimensionless. Similarly, the model provides experimental formulas for the calculation of Cl_i as a function of the patient's physical characteristics (weight, height, age and genre). Even in this case these quantities are considered dimensionless, with $Weight$ expressed in kg and $Height$ in cm.

$$\begin{aligned} Cl_1 &= 1.89 + 0.0456(Weight - 77) - 0.0681(lbm - 59) + 0.0264(Height - 177) \\ Cl_2 &= 1.29 - 0.024(Age - 53) \\ Cl_3 &= 0.836 \end{aligned} \tag{1.4}$$

The term lbm in (1.4) represents the *lean body mass*[3], which is calculable using the **James Formula**:

$$\begin{aligned} lbm &= 1.1Weight - 128\frac{Weight^2}{Height^2} \quad \text{Men;} \\ lbm &= 1.07Weight - 148\frac{Weight^2}{Height^2} \quad \text{Women.} \end{aligned} \tag{1.5}$$

[1] "The removal of a substance from the blood, expressed as the volume of blood or plasma cleared of the substance per unit time."The American Heritage® Medical Dictionary Copyright© 2007, 2014.

[2] With respect to the expressions present in literature, we decided to operate a normalization of the coefficient, in order to express $u(t)$ in $[mass/s]$.

[3] It is a coefficient that represents the difference between the total mass of the body and fat mass.

To know the concentration in the primary compartment:

$$y(t) = C_p(t) = \frac{q_1(t)}{V_1}[mass/l] \tag{1.6}$$

In the usage domain[4] it is possible to consider the model as Linear Time Invariant (LTI) and therefore obtain the state-space representation:

$$\begin{cases} \dot{x}(t) = \mathbf{A}x(t) + \mathbf{B}u(t) \\ y(t) = \mathbf{C}x(t) + \mathbf{D}u(t) \end{cases} \tag{1.7}$$

having state matrix:

$$\mathbf{A} = \begin{pmatrix} -(k_{10} + k_{12} + k_{13}) & k_{21} & k_{31} \\ k_{12} & -k_{21} & 0 \\ k_{13} & 0 & -k_{31} \end{pmatrix}; \tag{1.8}$$

with input, output and direct matrices:

$$\mathbf{B} = \begin{pmatrix} 1 & 0 & 0 \end{pmatrix}^T; \quad \mathbf{C} = \begin{pmatrix} \frac{1}{V_1} & 0 & 0 \end{pmatrix}; \quad \mathbf{D} = 0. \tag{1.9}$$

Applying the Laplace transform to the system represented in the state-space form, gives the following transfer function:

$$\frac{Y}{U} = G_{Cp,u}(\mathbf{s}) = K\frac{\left(1 + \frac{\mathbf{s}}{z_1}\right)\left(1 + \frac{\mathbf{s}}{z_1}\right)}{\left(1 + \frac{\mathbf{s}}{p_1}\right)\left(1 + \frac{\mathbf{s}}{p_2}\right)\left(1 + \frac{\mathbf{s}}{p_3}\right)}; \tag{1.10}$$

where p_i are the eigenvalues of the state matrix, K e z_i are the gain and the resulting zeros. The output of (1.7) and(1.10) is the plasma concentration of the SISO model considering only the propofol.

[4]It is assumed (plausible) that there are negligible mass variations during the operation.

Pharmacodynamics of propofol

The pharmacodynamics is characterized by a first-order relation with no delay that binds the concentration of the drug in the central compartment (C_p) with a fictitious one, called *Effect-Side-Compartment*, in which $C_e(t)$ is thought as the actual concentration in the patient's cerebral cortex. This compartment is significantly smaller than the rest of the body and is almost constant for all individuals [19]. The the effect-side-compartment concentration can be calculated, since k_{e0} will precisely characterize the temporal effects of equilibration between the plasma concentration and the corresponding drug effect:

$$\dot{C}_{e,p}(t) = k_{e0}(C_p(t) - C_e(t)); \tag{1.11}$$

The value of k_{e0} has been estimated in literature [19] and can be obtained as follows:

$$k_{e0} = 0.459/60 = 0.00765\ [s^{-1}]. \tag{1.12}$$

The presence of this Effect-Side-Compartment is due to the presence of a delay between plasma concentration in the blood and clinical effect. This behavior was validated by analyzing blood samples during anesthesia to compare the drug concentration in the primary compartment with the DoH measured by an EEG monitor.

Nonlinear interaction

EEG monitors are used to relate drug concentration with the clinical effect, with the aim of evaluating patients anesthesia level. EEG is a very noisy signal and presents difficulties in the interpretation: for these reasons it is preferred to use other systems that automatically process the EEG signal. One of these is the Bispectral Index Scale (BIS), a dimensionless parameter that can vary from 0 and 100, indicating respectively the situation of flat EEG and completely awake patient.
The relationship between plasma concentration and BIS can be expressed mathematically using a non-linear sigmoid surface, also known as *Hill function*. In this paragraph it is

considered the use of only propofol and the surface is reduced to a curve, expressed by the relation:

$$BIS(t) = E_0 - E_{max}\left(\frac{C_e(t)^\gamma}{C_e(t)^\gamma + C_{e_{50}}(t)^\gamma}\right); \tag{1.13}$$

where:

- E_0 indicates the initial state of the BIS without patient infusion;
- $E_{max} - E_0$ represents the maximum effect achievable by the infusion;
- γ denotes the steepness of the curve, that is the patient's receptivity to drugs;
- $C_{e_{50}}$ is the drug concentration needed to reach half the maximum effect. It is related to the sensitivity of pharmacokinetics;
- $C_e(t)$ expresses the concentration in the effect-site over the time.

As shown in figure 1.5 the Hill function is strongly non-linear and is characterized by the presence of an initial and a final saturation. At the beginning of the infusion, in fact, the curve presents a *plateau*, where small amounts of drug in the plasma concentration have no clinical effect until they reach a certain value. The final saturation expresses the impossibility of the level of hypnosis to overcome the maximum value allowed by E_{max}, regardless of the amount of drug infused.

1.3.2 MISO model

The SISO model previously illustrated relates the infusion profile of the hypnotic drug propofol with the clinical effects on the patient, measured by the BIS index. However during a surgical operation are also administered medication for muscle relaxation and analgesics. An estimate of the level of myoresolution can be performed using the electromyography (EMG). A lot of studies have been made on the subject [14, 21, 22] but a detailed analysis of the model goes beyond the objectives of this text, as drugs that block neuromuscular function do not affect the level of hypnosis of the patient (and therefore the BIS).

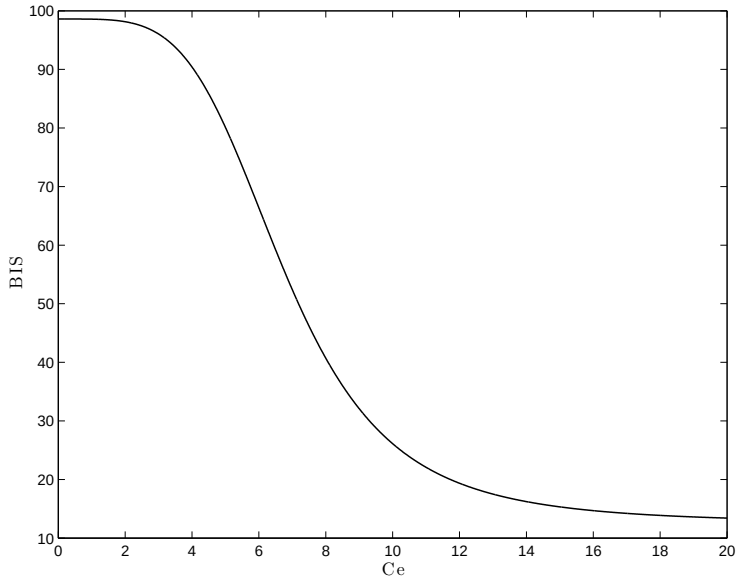

Figure 1.5: Graphic representation of the Hill function.

On the other hand, analgesic drugs like the remifentanil have a synergistic effect with propofol on the patient's hypnosis level [23, 24, 25]. It is therefore essential to study a model that describes the body's response to these drugs, using compartmentalized models and exploiting the pharmacokinetic and pharmacodynamic concepts already presented in the case of propofol alone (SISO model).
From the practical point of view, the synergistic effect translates into a reduction in the amount of propofol necessary to reach a certain level of anesthesia, with just a small infusion of remifentanil. In the literature it has been shown that the BIS is able to provide a quantitative evaluation of both drugs [26].

From a mathematical point of view it is necessary to construct a Multiple Input Single Output (MISO) model that has as inputs $u_{prop}(t)$ and $u_{remif}(t)$ and as output the DoH measured through the BIS. In this model the pharmacokinetics of propofol illustrated in section 1.3.1 will be left unchanged since remifentanil has a faster dynamics than propofol. Clinical studies [24] have shown that the action and absorption of remifentanil do not interact with propofol pharmacokinetics.
To take into account the combined effect of the two drugs, it will be necessary to construct

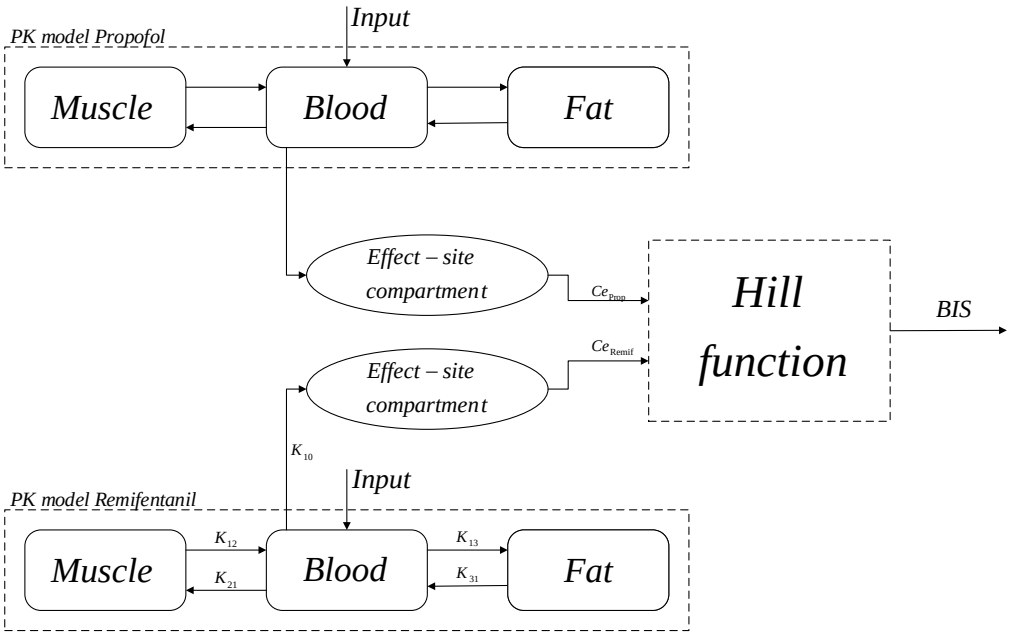

Figure 1.6: A schematic representation of a three compartmental PKPD model of the patient.

a more complex pharmacodynamic model with a Hill function that provides the level of BIS as a function of the concentrations of both drugs, as shown in figure 1.6. In this case it becomes a surface in space instead of the curve of the SISO model.

Pharmacokinetics of remifentanil

In the literature there are several models that describe the effects of the analgesic drug remifentanil on the level of anesthesia. In particular, the three-compartment model of Minto [20] has been studied and developed in depth. As already developed for propofol in section 1.3.1, it must be modelled an LTI system in the state-space as a function of coefficients k_{ij} which depend on V_i and Cl_i. The equations of the model are presented below:

$$\begin{aligned} k_{10} &= \frac{Cl_1}{60V_1}; \quad k_{12} = \frac{Cl_2}{60V_1}; \quad k_{13} = \frac{Cl_3}{60V_1}; \\ k_{21} &= \frac{Cl_2}{60V_2}; \quad k_{31} = \frac{Cl_3}{60V_2}. \end{aligned} \tag{1.14}$$

where V_i $[l]$ and Cl_i $[l/s]$ are the volume and the clearance of the compartment.

$$\begin{aligned} Cl_1 &= 2.6 - 0.0162(Age - 40) + 0.0191(lbm - 55); \\ Cl_2 &= 2.05 - 0.0301(Age - 40); \\ Cl_3 &= 0.076 - 0.00113(Age - 40). \end{aligned} \tag{1.15}$$

$$\begin{aligned} V_1 &= 5.1 - 0.0201(Age - 40) + 0.072(lbm - 55); \\ V_2 &= 9.82 - 0.0811(Age - 40) + 0.108(lbm - 55); \\ V_3 &= 5.42. \end{aligned} \tag{1.16}$$

As in the case of propofol, the lbm coefficients are extracted from the James formula (1.5). The compartmental model can be expressed using the generic representation in the state space (1.18) or by transfer function, in the same form as (1.10). The output of both representations is the plasma concentration of remifentanil C_r.

$$\begin{cases} \dot{x}(t) = \mathbf{A}x(t) + \mathbf{B}u(t) \\ y(t) = \mathbf{C}x(t) + \mathbf{D}u(t). \end{cases} \tag{1.17}$$

$$\mathbf{A} = \begin{pmatrix} -(k_{10} + k_{12} + k_{13}) & k_{21} & k_{31} \\ k_{12} & -k_{21} & 0 \\ k_{13} & 0 & -k_{31} \end{pmatrix}. \tag{1.18}$$

$$\mathbf{B} = \begin{pmatrix} 1 & 0 & 0 \end{pmatrix}^T; \quad \mathbf{C} = \begin{pmatrix} \frac{1}{V_1} & 0 & 0 \end{pmatrix}; \quad \mathbf{D} = 0. \tag{1.19}$$

Pharmacodynamics of remifentanil

The pharmacodynamics of remifentanil, as for propofol, is represented by a first-order function without delay that relates the plasma concentration of the analgesic $C_{e,r}$ of the first compartment with a fictitious one, called effect-site compartment. It approximates the delay between the plasma concentration of remifentanil in the blood with the hypnotic effect. With the hypothesis that this compartment has negligible dimensions compared to the rest of the system, we obtain the equation:

$$\dot{C}_{e,r}(t) = k_{e0,r} \left(C_r(t) - C_{e,r}(t) \right), \tag{1.20}$$

where C_r is the plasmatic concentration of remifentanil in the blood and $C_{e,r}$ is the effect-site compartment concentration:

$$C_{e,r} = \frac{q_{1,r}}{V_{1,r}}. \tag{1.21}$$

$V_{1,r}$ and $q_{1,r}$ are, respectively, the volume of the central compartment and the quantity of remifentanil in the central compartment. The concentration of remifentanil in the effect-site compartment can be completely calculated from the knowledge of the metabolism of the drug, described by the parameter $k_{e0,r}$ $[s^{-1}]$, which characterizes the balance time constant between plasma concentration and the corresponding effects of the drug. Its value has been estimated in literature [20] and depends on the age of the patient in question from the relation:

$$k_{e0,r} = 0.595 - 0.007 * (Age - 40) \tag{1.22}$$

Nonlinear interaction

The pharmacodynamics of remifentanil contemplate, in addition to the linear function of the first order presented above, a nonlinear static function that correlates the concentrations of propofol and remifentanil drugs in the human body with the measurable hypnotic effect. The relationship is known as a *Hill function* and for simultaneous administration of propofol and remifentanil is a nonlinear surface that indicates the DoH through the

Bispectral Index Scale (BIS).

A widely accepted model for the interaction between propofol and remifentanil is proposed in [20]. The formulation requires the normalization of the effect-site concentrations of the drugs with respect to the concentrations needed to reach half of the maximum effect:

$$U_{prop}(t) = \frac{C_{e,p}(t)}{C_{e_{50},p}}, \quad U_{remif}(t) = \frac{C_{e,r}(t)}{C_{e_{50},r}}, \tag{1.23}$$

where:

- $C_{e,p}(t)$ and $C_{e,r}(t)$ are the effect-site concentrations of propofol and remifentanil coming from the first order linear model;

- $C_{e_{50},p}$ and $C_{e_{50},r}$ are the propofol and remifentanil concentration required to reach half of the maximum effect over the BIS level.

The interaction between propofol and remifentanil is super-additive, which means that their combined effect is greater than the sum of the single one. So the power of the combination of drugs is considered by the parameter ϕ, a dimensionless variable calculated as:

$$\phi = \frac{U_{prop}(t)}{U_{prop}(t) + U_{remif}(t)}, \tag{1.24}$$

By definition, ϕ ranges from 0 (remifentanil only) to 1 (propofol only). According to [25], it is necessary to introduce a new term in order to normalize the combined effect of the drugs:

$$U_{50}(\phi) = 1 - \beta\phi + \beta\phi^2. \tag{1.25}$$

β correlates the action of the drug with the number of units associated with 50% of the maximum effect. The increase of β implies a greater hypnotic effect due to the synergistic effect of drugs.

Finally, the concentration-response relationship for any ratio of the two drugs can be

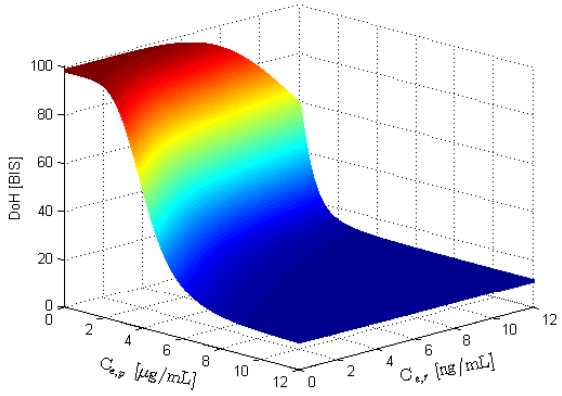

Figure 1.7: Hill Surface representing the response of patients to the simultaneous infusion of propofol and remifentanil.

described as:

$$BIS(t) = E_0 - E_{max} \left(\frac{\left(\frac{U_{prop}(t) + U_{remif}(t)}{U_{50}(\phi)} \right)^{\gamma}}{1 + \left(\frac{U_{prop}(t) + U_{remif}(t)}{U_{50}(\phi)} \right)^{\gamma}} \right) \tag{1.26}$$

where:

- E_0 is the initial state of the partient, without any infusion;
- $E_{max} - E_0$ represents the maximum reachable effect;
- γ denotes the steepness of the curve, that is the patient's receptivity to drugs;
- U_{prop} and U_{remif} are propofol and remifentanil concentrations normalized with respect to half of the maximum. They are connected with clinical sensitivity to drugs;
- $U_{50}(\phi)$ expresses the power of both drugs at the ϕ ratio as the number of units associated with the 50% of the maximum effect.

The Hill surface is influenced by the parameters $C_{e,p}$ e $C_{e,r}$ and the typical trend is shown in figure 1.7, where the curve is represented for $C_{e,p}$ and $C_{e,r}$ varying in the range $0 - 12$ $[\mu g/mL]$ and $0 - 12$ $[ng/mL]$ respectively ($E_0 = 98.0$, $E_{max} = 87.0$, $C_{e_{50}} = 4.12$, $C_{e_{50}} = 12.50$, $\gamma = 5.21$, $\beta = 1$). Similar to the Hill curve, the Hill surface is strongly non-linear and presents an initial and a final saturation: the plateau at the beginning of

the infusion indicates that small amounts of drug in the body do not involve significant clinical effects until they exceed a certain threshold. The final saturation region expresses the impossibility of the drugs effect to exceed the maximum achievable value expressed by E_{max}, regardless of the amount of drug infused.

1.3.3 Clinical data

After presenting the structure of the models that describe the response of the human body to the infusion of propofol and remifentanil drugs, it is necessary to have a database of patient data to define the parameters of the models. We use a population of 12 clinical cases present in the literature [13]. For each patient the physical characteristics (age, sex, height, weight) and the parameters of the Hill function have been indicated (E_0, E_{max}, $C_{e_{50}}$, γ)[5]. These data are useful for a preliminary analysis of the system and for the development of a propofol infusion-only controller. Furthermore, an additional patient, called the average patient, has been calculated, whose Hill parameters and physical characteristics are obtained as the mean of the corresponding data of the 12 patients. This case will be useful for considering medium dynamics in the patients database. The population is shown in the table 1.1.

In order to define the complete model considering the synergistic effect of drugs, a normal distribution of the two parameters $\beta = 1.5$ and $C_{e_{50},r} = 12.5$ $[ng/ml]$ found in literature [13, 27] was created to artificially reproduce the intra-patient variability of real cases. Thus, a population of 12 patients is available, with all the parameters necessary to building the complete MISO model presented before. Also in this case an average patient with average characteristics of the population has been created. Table 1.2 contains the data.

[5]These parameters have been estimated by analyzing the propofol infusion response only

Id	**Age**	**Height [cm]**	**Weight [kg]**	**Gender**	$C_{e_{50}}$	γ	E_0	E_{max}
1	40	163	54	F	6.33	2.24	98.8	94.10
2	36	163	50	F	6.76	4.29	98.6	86.00
3	28	164	52	F	8.44	4.10	91.2	80.70
4	50	163	83	F	6.44	2.18	95.9	102.00
5	28	164	60	M	4.93	2.46	94.7	85.30
6	43	163	59	F	12.00	2.42	90.2	147.00
7	37	187	75	M	8.02	2.10	92.0	104.00
8	38	174	80	F	6.56	4.12	95.5	76.40
9	41	170	70	F	6.15	6.89	89.2	63.80
10	37	167	58	F	13.70	1.65	83.1	151.00
11	42	179	78	M	4.82	1.85	91.8	77.90
12	34	172	58	F	4.95	1.84	96.2	90.80
13	38	169	65	F	7.42	3.00	93.1	96.58

Table 1.1: Patient database for propofol-only infusion models.

Id	**Age**	**Height [cm]**	**Weight[kg]**	**Gender**	$\mathbf{C_{e_{50},p}}$	$\mathbf{C_{e_{50},r}}$	γ	β	$\mathbf{E_0}$	$\mathbf{E_{max}}$
1	40	163	54	F	6.33	12.5	2.24	2.00	98.8	94.10
2	36	163	50	F	6.76	12.7	4.29	1.50	98.6	86.00
3	28	164	52	F	8.44	7.1	4.10	1.00	91.2	80.70
4	50	163	83	F	6.44	11.1	2.18	1.30	95.9	102.00
5	28	164	60	M	4.93	12.5	2.46	1.20	94.7	85.30
6	43	163	59	F	12.00	12.7	2.42	1.30	90.2	147.00
7	37	187	75	M	8.02	10.5	2.10	0.80	92.0	104.00
8	38	174	80	F	6.56	9.9	4.12	1.00	95.5	76.40
9	41	170	70	F	6.15	11.6	6.89	1.70	89.2	63.80
10	37	167	58	F	13.70	16.7	3.65	1.90	83.1	151.00
12	42	179	78	M	4.82	14.0	1.85	1.20	91.8	77.90
12	34	172	58	F	4.95	8.8	1.84	0.90	96.2	90.80
13	38	169	65	F	7.42	10.5	3.00	1.00	93.1	96.58

Table 1.2: Patient database for the propofol-remifentanil combined infusion models.

Chapter 2

Materials and methods

This chapter presents the technologies subsequently used in the implementation of the anesthesia control system. We will illustrate the type of controller that we want to implement for the regulation of propofol, focusing on the problems, characteristics and innovations introduced. In this general introduction it is important to remember the final application of the control structure: it considers the patient's BIS level as a process output, the propofol dosage as the control variable and the desired BIS value as the set-point.

We will begin by briefly presenting the characteristics of the GPC controllers, at the base of the developed control structure. We will then go on to introduce the genetic algorithms used for calibration of the controllers and finally we will describe the Monte Carlo method used to generate a large patient database for testing the robustness of the controller.

2.1 Generalized predictive control

The GPC was first proposed by Clarke and co-workers [28, 29] in the 1987 and has become one of the most popular MPC methods. In fact it has been successfully implemented in many industrial applications [30], showing good performance also in terms of robustness. The GPC can handle many different control problems for a broad gamma of

plants with a reasonable number of design variables selected by the user depending by the control objectives and exploiting prior knowledge of the plant.

The GPC basic idea [31] consist in computing the future control signals in order to minimize a multistage cost function which is defined over the prediction horizon. The multistage cost function manage the trade-off between the control effort and the distance between the predicted system output and some predicted reference sequence over the horizon. GPC can deal with unstable and non-minimum phase plants and in case of absence of constrains it provides an analytical solution to the computation of the control signal.

The general options available for GPC leads to a greater variety of control objectives compared to other approaches, some of which can even be considered as limiting case of GPC.

2.1.1 Formulation of Generalized Predictive Control

Most SISO plants, when considering operation around a particular operating point can be linearized and described by:

$$A(z^{-1})y(k) = z^{-d}B(z^{-1})u(k-1) + C(z^{-1})\varepsilon(k)$$

where $u(k)$ is the control sequence, $y(k)$ the output sequence of the plant and $\varepsilon(k)$ is the zero mean white noise. A, B and C are the following polynomials, in the backward shift operator z^{-1}:

$$A(z^{-1}) = 1 + a_1 z^{-1} + a_2 z^{-2} + ... + a_{na} z^{-na}$$

$$B(z^{-1}) = b_0 + b_1 z^{-1} + b_2 z^{-2} + ... + b_{nb} z^{-nb}$$

$$C(z^{-1}) = 1 + c_1 z^{-1} + c_2 z^{-2} + ... + c_{nc} z^{-nc}$$

where d is the dead time of the system. This model is known as a Controller Auto-Regressive Moving-Average (CARMA) model. It has been argued [28] that for many industrial applications in which the disturbances are non-stationary an integrated CARMA

(CARIMA) is more appropriate. A CARIMA model is described by:

$$A(z^{-1})y(k) = z^{-d}B(z^{-1})u(k-1) + C(z^{-1})\frac{\varepsilon(k)}{\Delta} \tag{2.1}$$

with

$$\Delta = 1 - z^{-1}$$

For simplicity in the following, the C polynomial is chosen to be 1. In this way C^{-1} can be truncated and absorbed into A and B [31].

The GPC multistage cost function can be written as:

$$J = \sum_{j=N_1}^{N_2} \delta(j)[\hat{y}(k+j|k) - w(k+j)]^2 + \sum_{j=1}^{N_u} \lambda(j)[\Delta u(k+j-1)]^2 \tag{2.2}$$

where $\hat{y}(k+j|k)$ is an optimum j step ahead prediction of the system output computed at the discrete time k , N_1 and N_2 are the minimum and maximum prediction horizons, N_u is the control horizon, $w(k+j)$ is the future reference trajectory and $\delta(j)$ and $\lambda(j)$ are used as weight to handle the trade-off between the control effort and the trajectory following.

The aim of predictive control is to compute the future control actions $u(k), u(k+1), ...,$ in such a way that the future system output $y(k+j)$ is driven close to $w(k+j)$. This is accomplished by minimizing J, the expectation of (2.2).
In order to optimize the cost function, the optimal prediction of $y(k+j)$ for $j \geq N_1$ to $j \leq N_2$ must be obtained. Consider the following Diophantine equation:

$$1 = E_j(z^{-1})\tilde{A}(z^{-1}) + z^{-j}F_j(z^{-1}) \text{ with } \tilde{A}(z^{-1}) = \Delta A(z^{-1}) \tag{2.3}$$

The E_j and F_j polynomials are uniquely defined with degrees $j-1$ and na, respectively [31]. They can be obtained dividing 1 by $\tilde{A}(z^{-1})$ until the reminder can be factorized as $z^{-j}F_j(z^{-1})$. The quotient of the division is the polynomial $E_j(z^{-1})$.

If (2.1) is multiplied by $\Delta E_j(z^{-1})z^j$ we obtain:

$$\tilde{A}(z^{-1})E_j(z^{-1})y(k+j) = E_j(z^{-1})B(z^{-1})\Delta u(k+j-d-1) + E_j(z^{-1})\varepsilon(k+j) \qquad (2.4)$$

Considering (2.3), (2.4) can be written as:

$$(1 - z^{-j}F_j(z^{-1}))y(k+j) = E_j(z^{-1})B(z^{-1})\Delta u(k+j-d-1) + E_j(z^{-1})\varepsilon(k+j)$$

which in turn can be rewritten as:

$$y(k+j) = F_j(z^{-1})y(k) + E_j(z^{-1})B(z^{-1})\Delta u(k+j-d-1) + E_j(z^{-1})\varepsilon(k+j) \qquad (2.5)$$

The degree of polynomial $E_j(z^{-1}) = j-1$ and the noise terms in (2.5) are all in the future. The best prediction of $y(k+j)$ is therefore:

$$y(k+j) = G_j(z^{-1})\Delta u(k+j-d-1) + F_j(z^{-1})y(k)$$

where $G_j(z^{-1}) = E_j(z^{-1})B(z^{-1})$.

It is possible to show that the polynomials E_j and F_j have been obtained dividing 1 by $\tilde{A}(z^{-1})$ until the remainder of the division can be factorized as $z^{-j}F_j(z^{-1})$. These polynomial can be expressed as:

$$F_j(z^{-1}) = f_{j,0} + f_{j,1}z^{-1} + ... + f_{j,na}z^{-na}$$

$$E_j(z^{-1}) = e_{j,0} + e_{j,1}z^{-1} + ... + e_{j,j-e}z^{-(j-1)}$$

The same procedure is used to obtain E_{j+1} and F_{j+1} that is dividing 1 by $\tilde{A}(z^{-1})$ until the reminder of the division can be factorized as $z^{-(j+1)}F_{j+1}(z^{-1})$, with

$$F_{j+1}(z^{-1}) = f_{j+1,0} + f_{j+1,1}z^{-1} + ... + f_{j+1,na}z^{-na}$$

At this point only another step of the division performed to obtain the polynomials E_j and F_j has to be taken into account to obtain the polynomials E_{j+1} and F_{j+1}. The polynomial E_{j+1} will be given by:

$$E_{j+1}(z^{-1}) = E_j(z^{-1}) + e_{j+1,j}z^{-j}$$

with $e_{j+1,j} = f_{j,0}$

The coefficient of polynomial F_{j+1} can be expressed as:

$$f_{j+1,i} = f_{j,i+1} - f_{j,i+1}\tilde{a}_{i+1},\ i = 0, \ldots, na-1$$

The polynomial G_{j+1} can be obtained recursively as follows:

$$G_{j+1} = E_{j+1}B = (E_j + f_{j,0}z^{-j})B$$

$$G_{j+1} = G_j + f_{j,0}z^{-j}B$$

It is possible to notice that the first j coefficient of G_{j+1} will be identical to those of G_j and the remaining coefficients will be given by:

$$g_{j+1,j+i} = g_{j,j+i} + f_{j,0}b_i$$

To solve the GPC problem the set of control signals $u(k), u(k+1), ..., u(k+N_u)$ has to be obtained in order to optimize (2.2). Because the considered system has a dead time of d sampling periods, the output of the system will be influenced by signal $u(k)$ only after $d+1$ sampling periods. The prediction and control horizons can be defined by $N_1 = d+1$, $N_2 = d+N$ and $N_u = N$. Notice that there is no point in making $N_1 < d+1$ as terms added to (2.2) will only depend on the past control signal. On the other hand, if $N_1 > d+1$ the first points in the reference sequence, which is the ones guessed with most certainty, will not be taken into account.

Now considering the following set of j ahead optimal predictions:

$$\hat{y}(k+d+1|k) = G_{d+1}\Delta u(k) + F_{d+1}y(k)$$

$$\hat{y}(k+d+2|k) = G_{d+2}\Delta u(k+1) + F_{d+2}y(k)$$

$$\vdots$$

$$\hat{y}(k+d+N|k) = G_{d+N}\Delta u(k+N-1) + F_{d+N}y(k)$$

it can be written as [31]:

$$\mathbf{y} = \mathbf{G}\mathbf{u} + \mathbf{F}(z^{-1})y(k) + \mathbf{G}'(z^{-1})\Delta u(k-1) \tag{2.6}$$

where

$$\mathbf{y} = \begin{bmatrix} \hat{y}(k+d+1|k) \\ \hat{y}(k+d+2|k) \\ \vdots \\ \hat{y}(k+d+N|k) \end{bmatrix}$$

$$\mathbf{u} = \begin{bmatrix} \Delta u(k) \\ \Delta u(k+1) \\ \vdots \\ \Delta u(k+N-1) \end{bmatrix}$$

$$\mathbf{G} = \begin{bmatrix} g_0 & 0 & \dots & 0 \\ g_1 & g_0 & \dots & 0 \\ \vdots & \vdots & \vdots & \vdots \\ g_{N-1} & g_{N-2} & \cdots & g_0 \end{bmatrix}$$

$$\mathbf{G}'(z^{-1}) = \begin{bmatrix} (G_{d+1}(z^{-1}) - g_0)z \\ (G_{d+2}(z^{-1}) - g_0 - g_1 z^{-1})z^2 \\ \vdots \\ (G_{d+N}(z^{-1}) - g_0 - g_1 z^{-1} - \ldots - g_{N-1}z^{-(N-1)})z^N \end{bmatrix}$$

$$\mathbf{F} = \begin{bmatrix} F_{d+1}(z^{-1}) \\ F_{d+2}(z^{-1}) \\ \vdots \\ G_{d+N}(z^{-1}) \end{bmatrix}$$

Notice that the last two terms in (2.6) only depend on the past and can be grouped into **f**:

$$\mathbf{y} = \mathbf{G}\mathbf{u} + \mathbf{f}$$

If all initial conditions are zero, the free response **f** is also zero. If a unit step is applied to the input at time k:

$$\Delta u(k) = 1,\ \Delta u(k+1) = 0, \ldots, \Delta u(k+N-1) = 0$$

the expected output sequence $[\hat{y}(k+1), \hat{y}(k+2), \ldots, \hat{y}(k+N)]^T$ is equal to the first column of matrix **G**. In this way it is possible to calculate the first column of matrix **G** as the step response of the process when a unit step is applied to the manipulated variable. The free response term can be calculated recursively by:

$$f_{j+1} = z(1 - \tilde{A}(z^{-1})f_j + B(z^{-1})\Delta u(k-d+j)$$

with $f_0 = y(k)$ and $\Delta u(k+j) = 0$ for $j \leq 0$.

Expression (2.2) can be written as

$$J = (\mathbf{G}\mathbf{u} + \mathbf{f} - \mathbf{w})^T(\mathbf{G}\mathbf{u} + \mathbf{f} - \mathbf{w}) + \lambda \mathbf{u}^T\mathbf{u} \tag{2.7}$$

where

$$\mathbf{w} = [w(k+d+1), w(k+d+2), \ldots, w(k+d+N)]^T$$

Equation (2.7) can be written as

$$J = \frac{1}{2}\mathbf{u}^T\mathbf{H}\mathbf{u} + \mathbf{b}^T\mathbf{u} + \mathbf{f}_0 \tag{2.8}$$

where

$$\mathbf{H} = 2(\mathbf{G}^T\mathbf{G} + \lambda\mathbf{I})$$

$$\mathbf{b}^T = 2(\mathbf{f} - \mathbf{w})^T\mathbf{G})$$

$$\mathbf{f}_0 = (\mathbf{f} - \mathbf{w})^T(\mathbf{f} - \mathbf{w})$$

Assuming that there are no constraints on the control signals, the minimum of J can be found by making the gradient of J equal to zero [31]:

$$\mathbf{u} = -\mathbf{H}^{-1}\mathbf{b} = (\mathbf{G}^T\mathbf{G} + \lambda\mathbf{I})^{-1}\mathbf{G}^T(\mathbf{w} - \mathbf{f}) \tag{2.9}$$

Notice that only the first element of vector Δu is the control signal actually sent to the process:

$$\Delta u(k) = \mathbf{K}(\mathbf{w} - \mathbf{f}) \tag{2.10}$$

where $\mathbf{K}$ is the first row of matrix $(\mathbf{G}^T\mathbf{G} + \lambda\mathbf{I})^{-1}\mathbf{G}^T$.
If there are no future predicted errors (i.e. $\mathbf{w} - \mathbf{f} = 0$) then there is no control move, as the desired reference will be reached with the free evolution of the process. However, in the other case, the control action will be incremented proportionally to the future error (with the factor $\mathbf{K}$). Notice that instead taking the action based on past errors, as is the case in conventional feedback controllers, it is taken with respect to future errors.

Only the first element of $\mathbf{u}$ is used and the calculation is repeated at the next sampling time. To obtain the solution, the GPC needs to compute the inversion of an $N \times N$ matrix, which requires a substantial amount of effort. To reduce the amount of computation needed, the control horizon is used, assuming that the expected control signals are going to be constant after $N_u < N$. This leads to the inversion of an $N_u \times N_u$ matrix, reducing the amount of computation, but restricts the optimality of the GPC.

2.2 Genetic algorithms

In the literature, unlikely for the Proportional-Integrative-Derivative control law (PID) controllers, there are no techniques to calibrate the parameters of a GPC controller. As the patients model are available, it is a bit of a trial and error with the calibration. In this contest the genetic algorithms can be helpful to find heuristic solutions that best solve the problem.

Genetic Algorithms (GA) is a global and stochastic research method inspired by the principle of natural selection and biological evolution theorized in 1859 by Charles Darwin. They operate on a population of potential solutions applying the principle of survival of the best, thus evolving towards a solution that will hopefully approximate how much as much as possible to the real solution of the problem. With each new generation, a new set of solutions is created by the selection process that, based on the level of fitness, selects the best members of the population and makes them evolve using a series of genetic operators derived from natural genetics. This process leads to a robust evolution towards individuals who are better suited to the environment, i.e. to the set of solutions that best respond to the problem placed in the beginning. In particular, the steps to describe how the genetic algorithms work are the following:

- **initialization**: it begins with the creation of an initial population with random characteristics, but in any case limited within a certain pre-established range of values;

- **evaluation**: in this step each member of the population is evaluated using a cost function that specifies the criterion useful for estimating the best element of the population. The criterion can be simple, to reduce the time of computation, or complex, if more references are taken into account;

- **selection**: the cost function allows the elimination of the worst members from the populations, i.e. those that less respect the established criterion, preserving the best ones. This is what happens in nature with natural selection: the next generation will

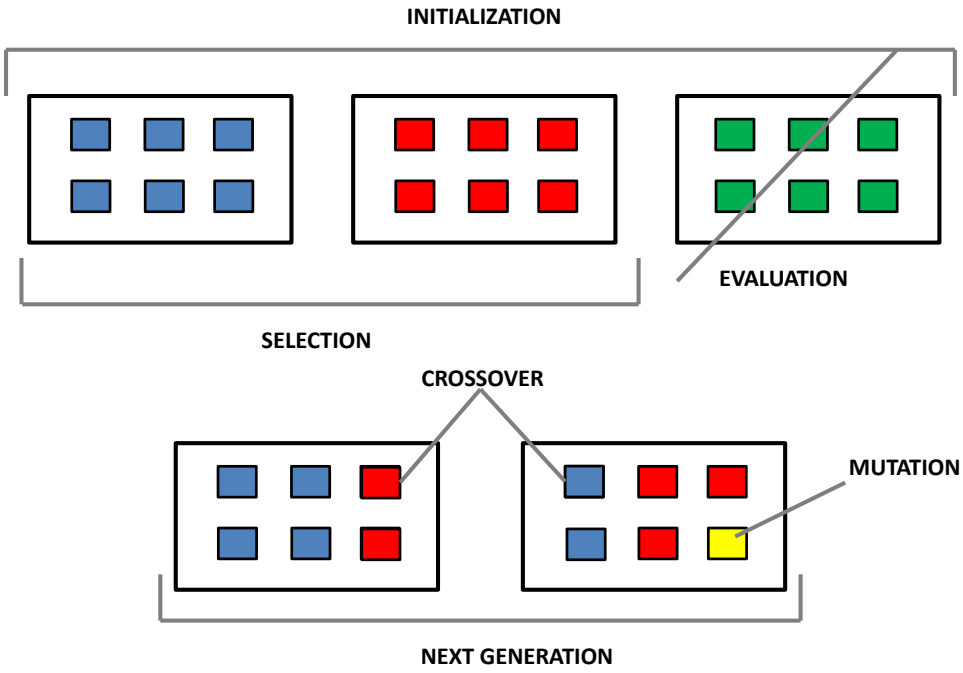

Figure 2.1: Schematic of the operation principle of genetic algorithms.

contain the best elements of the population;

- **crossover**: the characteristics of the selected elements are mixed in order to create new individuals. By doing this, it increases the probability that new individuals inherit the best characteristics from the old generation;

- **mutation**: it consists of a random behavior that is introduced into the new population. Usually this is achieved with small random variations to increase the chances of finding the optimal solution;

- **repetition**: after obtaining a new population, another iteration is made by repeating the previous steps. To stop the algorithm, a tolerance threshold is introduced between successive solutions.

In figure 2.1 an explanatory diagram of the functioning of genetic algorithms is represented. Genetic algorithms are often used in the field of artificial intelligence and computer science,

as they are a simple but very powerful tool for finding solutions to research problems; however, they also present some drawbacks. First there is the problem of initialization of the population, since if the initial parameters are not set correctly, the result will be unreliable. The second problem concerns the final solution found: the genetic algorithms ensure to find an optimal local solution, relative to the considered environment, which in some cases may not coincide with the global one. Both of these problems could be solved by imposing very large initial bounds and increasing the population, but this would result in a considerable increase in computational time.

In order to evaluate the best elements of the population, a fitness function is used, which provides as an index of adequacy the value of the IAE between the BIS and the reference signal:

$$IAE = \int_0^\infty |BIS(t) - r(t)|\, dt \tag{2.11}$$

In this way the selection process prefers the parameters that provide the lowest IAE. Just to give an example of the possible values of this index, in figure 2.2 are reported two different BIS profile with the relative IAE. It can be noticed that the red profile has a better trend, in fact, numerically speaking, the blue has an IAE of 4871 while the red one of 3340.

2.3 Monte Carlo method

Monte Carlo Method (MCM) or Monte Carlo experiments are a broad class of computational algorithms that rely on repeated random sampling to obtain numerical results. A Monte Carlo simulation is, in essence, the generation of random objects or processes by means of a computer. These objects could arise "naturally" as part of the modeling of a real-life system, such as a complex road network, the transport of neutrons, or the evolution of the stock market. In many cases, however, the random objects in Monte Carlo techniques are introduced "artificially" in order to solve purely deterministic problems. In this case the MCM simply involves random sampling from certain probability distributions. In either the natural or artificial setting of Monte Carlo techniques the idea is to repeat the

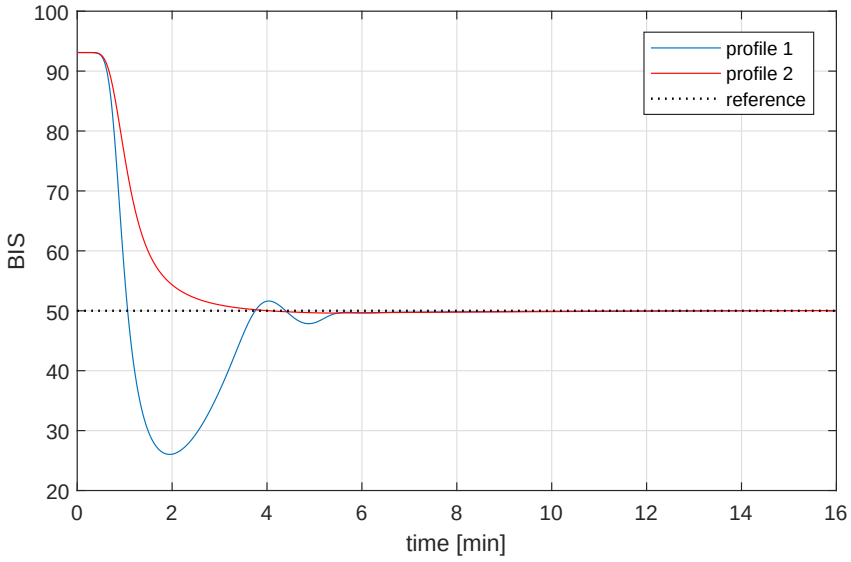

Figure 2.2: Example of two different BIS profile.

experiment many times (or use a sufficiently long simulation run) to obtain many quantities of interest using the *Law of Large Numbers* and other methods of statistical inference [32]. Here are some typical uses of the MCM:

- **Sampling**. Here the objective is to gather information about a random object by observing many realizations of it. An example is simulation modeling, where a random process mimics the behavior of some real-life system, such as a production line or telecommunications network. Another example is found in Bayesian statistics, where Markov chain Monte Carlo (MCMC) is often used to sample from a posterior distribution.

- **Estimation**. In this case the emphasis is on estimating certain numerical quantities related to a simulation model. An example in the natural setting of Monte Carlo techniques is the estimation of the expected throughput in a production line. An example in the artificial context is the evaluation of multi-dimensional integrals via Monte Carlo techniques by writing the integral as the expectation of a random variable.

- **Optimization**. The MCM is a powerful tool for the optimization of complicated objective functions. In many applications these functions are deterministic and randomness is introduced artificially in order to more efficiently search the domain of the objective function. Monte Carlo techniques are also used to optimize noisy functions, where the function itself is random - for example, the result of a Monte Carlo simulation.

The Monte Carlo method is thus an empirical method for evaluating statistics. Through computational "brute force", a researcher creates sampling distributions of relevant statistics. For that reason the MCM is used in this work to generate large samples of patients that would not be otherwise available. These samples will be used to test the robustness of the controller, because the controller will be initially tested only on the database of 13 patients presented in the first chapter and since that database does not cover all possible combinations, it is required an additional investigation on the behaviour of the controller in the presence of different patients. Detailed information about this topic will be provided in the future chapters. For further details of the Monte Carlo method, see [33], [34], or [35].

Chapter 3

Propofol infusion system

This chapter describes the implementation of the control technologies previously presented. In this preliminary phase the system for the infusion of propofol alone (SISO system) will be analyzed, thus neglecting the remifentanil and the synergistic effect of the two drugs. This is of fundamental importance for verifying the real possibility of developing an automatic system for anesthesia using the presented technology. It also allows the evaluation of the benefits offered by automatic control on a simpler system.
We will begin by presenting the implementation of the control structure of the SISO system, performing initial tests on patient models taken from the literature. This will allow the evaluation of the performance of the system in terms of adequacy to medical specifications. We will also test the robustness of the system by making further test on a database of randomly-generated patients.
Finally we will compare this predictive control structure with the use of a standard PID controller and other works present in the literature, evaluating the differences.

3.1 Control requirements

The control structure of the SISO system exploit the patient BIS signal as feedback and aim to reach the desired BIS level controlling the infusions of propofol. The goal is

therefore to create a controller that brings the patient's level of hypnosis to a desired value within a reasonable time frame.

From the medical specifications and the analysis of real infusion profiles provided by the Spedali Civili di Brescia, it is considered a reference BIS of 50 to be reached in about 120 $[s]$. This time is not so crucial, the anesthesiologist wants it as short as possible, but it is mandatory that the reference is reached within 300 $[s]$ to avoid risks on the patient. It is also important to note that the specification of the BIS at 50 is used to establish the set-point and it is not particularly binding: in fact the anesthesiologist considers acceptable the BIS values that ranges between 40 and 60.

In order to avoid risks to the health of the patient it is also important to avoid excessive variations of the BIS. For example during the initial transient, in which the patient goes from completely awake (BIS = 100) to unconscious (BIS = [60-40]), it is essential to limit the undershoot that lead the controlled variable to low and risky values. Finally, it is good practice to limit the use of drugs, that means trying to give the least amount of drug needed to achieve the desired level of anesthesia. This allows a better response of the patient in the post-operative phase and limits the side effects.

An additional specification to be considered concerns the minimum and maximum permissible infusion rates. This means that the control action must assume values within the established range. The minimum value is obviously 0 $[mg/s]$ and corresponds to the non-infusion situation of the drug: negative values of the control variable have no physical meaning, as they would represent a contrary flow of drug. The upper limit of infusion rates can be set at 4.00 or 6.67 $[mg/s]$. The first limit has been provided by clinical practice and represents the maximum rate used in boluses. The second value was instead calculated considering the maximum rate of a standard medical pump (*Graseby 3400, Smiths Medical, London, UK*) and the concentration of the hypnotic drug propofol (*Diprivan* 20 $[mg\ /\ ml]$) as:

$$Rate_{[mg/s]} = \frac{Rate_{[ml/h]}}{3600[s/h]} \cdot Concentration_{propofol} \tag{3.1}$$

In this work, we will consider the upper limit of 6.67 $[mg/s]$.

There is also another constraint that need to be taken into account: the maximum variations of the infusion rate, which is how faster the control variable can change. There are no practical values available but it is still possible to consider this constraint by avoiding too fast variations like peaks or wide oscillations on the control signal.
To summarize, the control specifications to be considered are shown in table 3.1.

Set-point reference	50
Undershoot	$10\%_{FS}$
Settling time	120 [s]
Upper limit	6.67 [mg/s]
Lower limit	0.0 [mg/s]

Table 3.1: Specifications of the SISO control system.

3.2 Control scheme

In figure 3.1 the control structure implemented using the technology presented in the previous chapter is shown. The control structure exploits the scheme proposed in [36] and allows the integration of the model of the patient in the control scheme to provide a personalized infusion of the drug. In the considered control architecture, $\tilde{P}$ is the PKPD linear model of the patients, and $\tilde{H}$ is the Hill function model. In particular, the parameters of $\tilde{P}$ can be easily computed for each patient, as described in section 1.3, using his/her demographic data. On the contrary, the parameters of the Hill function are generally unknown (with the exception of E_0 that can be measured for each patient) and the average parameters (13^{th} row of table 1.1) are used for all patients. The output of $\tilde{P}$ is the estimated effect site concentration $C_e(t)$ of the patient. In the ideal case, when the models $\tilde{P}$ and $\tilde{H}$ coincide with the patient dynamics P and H, the proposed scheme becomes a linear control system of the PKPD process. In fact, $\hat{r}$ is exactly the effect site concentration reference value corresponding to the desired BIS level $r(t)$. As it is shown in figure 3.1, $\hat{r}$ is simply calculated by the inversion of the static function $\tilde{H}$. In the ideal case, the model output $C_e(t)$ is the only feedback signal of the control scheme because the innovation

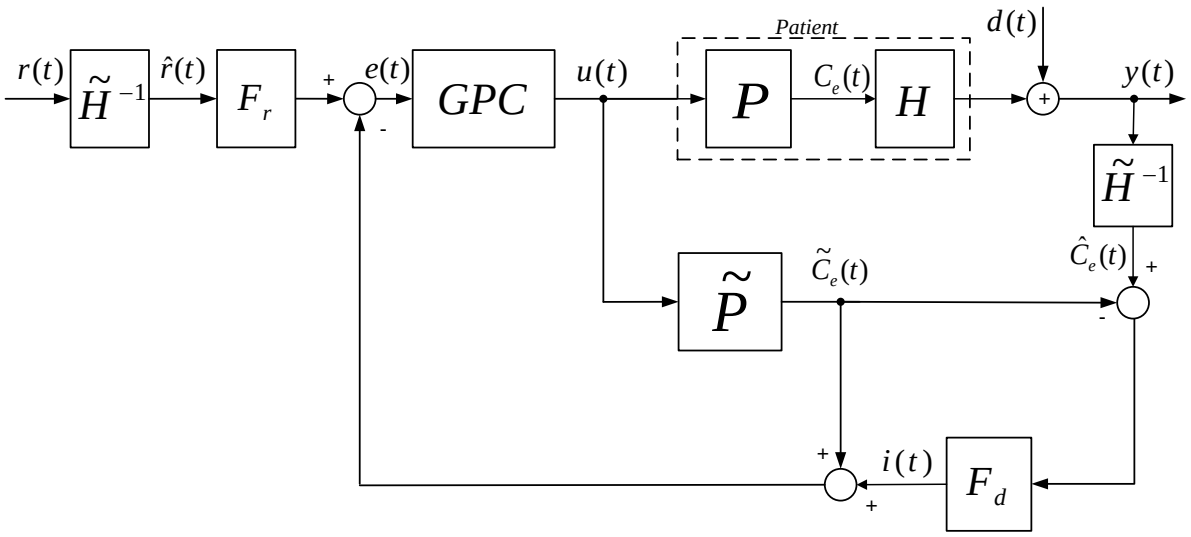

Figure 3.1: The SISO control scheme for the automatic regulation of propofol during anesthesia.

signal $i(t)$ is equal to zero since $C_e(t) = \hat{C}_e(t)$. In fact, $i(t)$ is different from zero only in the presence of disturbances on the process output that are not estimated by the internal model. However, the static nonlinearity in the Wiener model is always uncertain as it is virtually impossible to know the exact values of the parameters a priori. Moreover, also the linear PKPD model is uncertain due to the parameters variability. As mentioned above, in this paper we select $\tilde{H}$ by considering the average Hill function parameters found in [7] while $\tilde{P}$ changes for each patient based on his/her demographic data, as explained in section 1.3. The innovation signal $i(t)$ is therefore necessary to compensate for the differences between $\tilde{P}$ and P, between $\tilde{H}$ and H, and for the disturbances induced by noxious stimuli. The contribution of $i(t)$ depends on the error between the estimated effect site concentration $C_e(t)$ and the effect site concentration $\hat{C}_e(t)$ calculated using the BIS signal via average Hill function inversion $\tilde{H}^{-1}$. In particular, at the steady-state, the innovation signal allows the compensation of the possibly wrong reference signal $\hat{r}$ calculation. Indeed, the anesthesiologist fixes the BIS level reference and the inversion of the average Hill function $\tilde{H}$ defines the effect site concentration reference. However, $\hat{r}$ can be different from the $C_e(t)$ steady-state value necessary to reach the desired BIS level,

due to the difference between H and $\tilde{H}$. Nevertheless, the same estimated inverted Hill function $\tilde{H}^{-1}$ used to compute $\hat{r}$ is also fed back through the innovation guaranteeing zero steady-state tracking error even in the presence of uncertainties.
The blocks F_d and F_r in the scheme are two low-pass filters. The F_r filter is used to obtain a smooth reference profile, avoiding an aggressive response of the controller. As done in [37], this filter is used to achieve the desired set point response, leaving the controller focused on the disturbance rejection task. The transfer function is:

$$F_r(s) = \frac{1}{T_{fr}s + 1} \tag{3.2}$$

The filter F_d acts on the innovation signal $i(t)$ and handles the trade-off between the contribution of the innovation in the control system and the noise filtering action. Also F_d is selected as a first-order low-pass filter:

$$F_d(s) = \frac{1}{T_{fd}s + 1} \tag{3.3}$$

3.2.1 Tuning of the parameters

To be able to test the implemented control scheme, which means to study how the system responds to the set-point and how it behaves in the presence of disturbances, it is necessary to calibrate the controller appropriately. In order to obtain the best performances after some trial we decided to handle the set point following and disturbances rejection tasks separately. The controller will be tuned to maximise the performance in rejecting the disturbance, while the time constant of the filter T_r will be chosen to obtain a good set point response. The tuning is performed by means of the GA and it is divided into two phases: firstly the GPC controller is tuned considering the system without the filter and introducing the disturbances as two steps (one positive and the other negative). Then the filter time constant T_{fr} is found considering the already tuned GPC but focusing only on the set point response. The calibration is performed in both cases with the genetic algorithms that determine, through various cost functions, the best set of parameters of the

controller. For further information on the functioning of these algorithms refer to section 2.2.

As regards the calibration for the rejection of disturbances, it was necessary to introduce further constraints because otherwise the control variable presents too fast variations that cannot be followed in the reality. In fact, without these constraint, the manipulated variable is as pictured in figure 3.2 and presents high and fast oscillations at minute 6 and 11, when the disturbances occur. This happens because for the specific process, there exist issues. Analyzed system obtains steady state after approximately 9000 seconds. Following general rule for MPC design it is recommended that prediction horizon should be selected as approximately 60-70% of steady state time. With selected sampling time of 1 seconds this will results in very large GPC's internal matrixes, and in consequence it will be impossible to compute the solution in inter sampling time. The situation changes when the sampling time is set up to 180 seconds and prediction horizon is set up to 40 samples. For this configurations we obtained desired performance with small computational effort. Nevertheless, for the analyzed process such a big sampling time is not acceptable and we need to consider another approach. To obtain an acceptable trend of the manipulated variable it is necessary to introduce the following constraints:

- If $\Delta U > 0.5$ in one of the last 5 samples then the maximum allowed decrement of the manipulated variable (for the next calculation) it will be $\Delta U_{min} = -0.1$. This will compensate for positive disturbances preventing the controller output to decrement too fast.

- If the BIS signal is under the reference then the maximum allowed increment of the manipulated variable it will be $\Delta U_{max} = +0.1$. In this way when oscillations occur and the BIS is under the reference (negative disturbances) the manipulated variable is forced to stay at low levels until the BIS reaches the reference.

- In the other cases the ΔU_{min} and ΔU_{max} remains the highest possible, as there is no need to intervene.

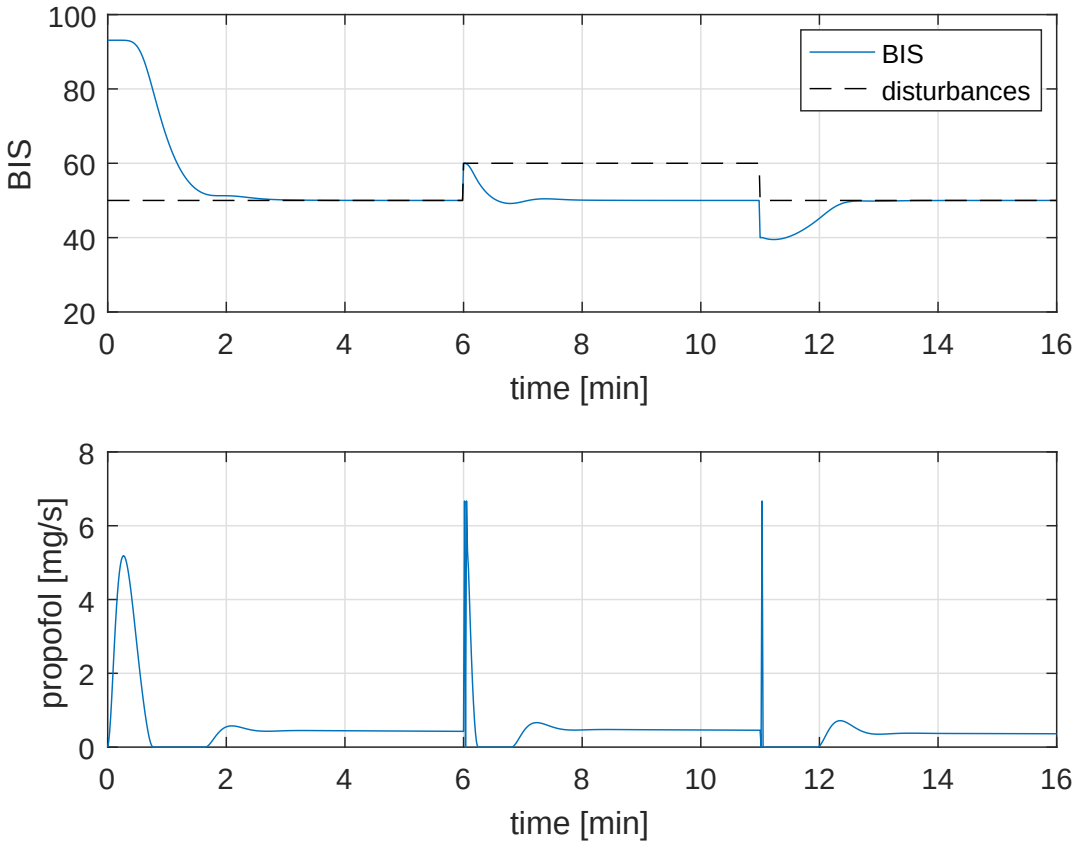

Figure 3.2: Response of the average 13 patient without constraints.

The controller output obtained with this new contrives results having an acceptable profile and also a better response in terms of performance indexes.

As a criterion for the cost function, IAE was chosen. It provides a measure of the behavior of the system by integrating the absolute value of the error variable:

$$IAE = \int |r(t) - BIS(t)|dt \tag{3.4}$$

The lower the IAE, the better the behavior of the system will be, because it means that there are less differences between the reference and the BIS.

The calibration parameters obtained from the execution of the genetic algorithms are reported in the table 3.2.

N	27
Nu	7
λ	1.6
Td	22.7
Tr	44.9

Table 3.2: Calibration parameter for the propofol only infusion system.

3.2.2 Simulations

After tuning the controller, it is now possible to analyze the response of the SISO system to the set-point of 50, with the calibration parameters of table 3.2. As a first illustrative result we consider the average patient 13 reported in table 1.1. It represents a fictitious patient, that is, its parameters are derived from the mean of the other patients. It can be considered as the average patient and therefore the one on which perform the first tests of the control structure. The patient is characterized by the following linear model:

$$PK(s) = \frac{0.2342s^2 + 0.001631s + 1.521 \cdot 10^{-6}}{s^3 + 0.02404s^2 + 9.904 \cdot 10^{-5}s + 4.726 \cdot 10^{-8}} \tag{3.5}$$

$$PD(s) = \frac{0.00765}{s + 0.00765} \tag{3.6}$$

in series with the non linear Hill function:

$$BIS(t) = 93.1 - 96.58 \left(\frac{C_e(t)}{C_e(t) + 7.42} \right)^3; \tag{3.7}$$

The simulation results of the induction and maintenance phases are shown in figure 3.3. The BIS signal is plotted in the top part of the figure while the control action is plotted in the bottom part. The performance achieved with the average patient is satisfactory from the clinical point of view. In fact, the BIS level attains the set-point reference without undershoot and with an acceptable settling time. More in details, the following performance indexes, proposed in [13], have been calculated for the set-point following (namely, the induction phase) task in order to evaluate the performance of the automatic control system:

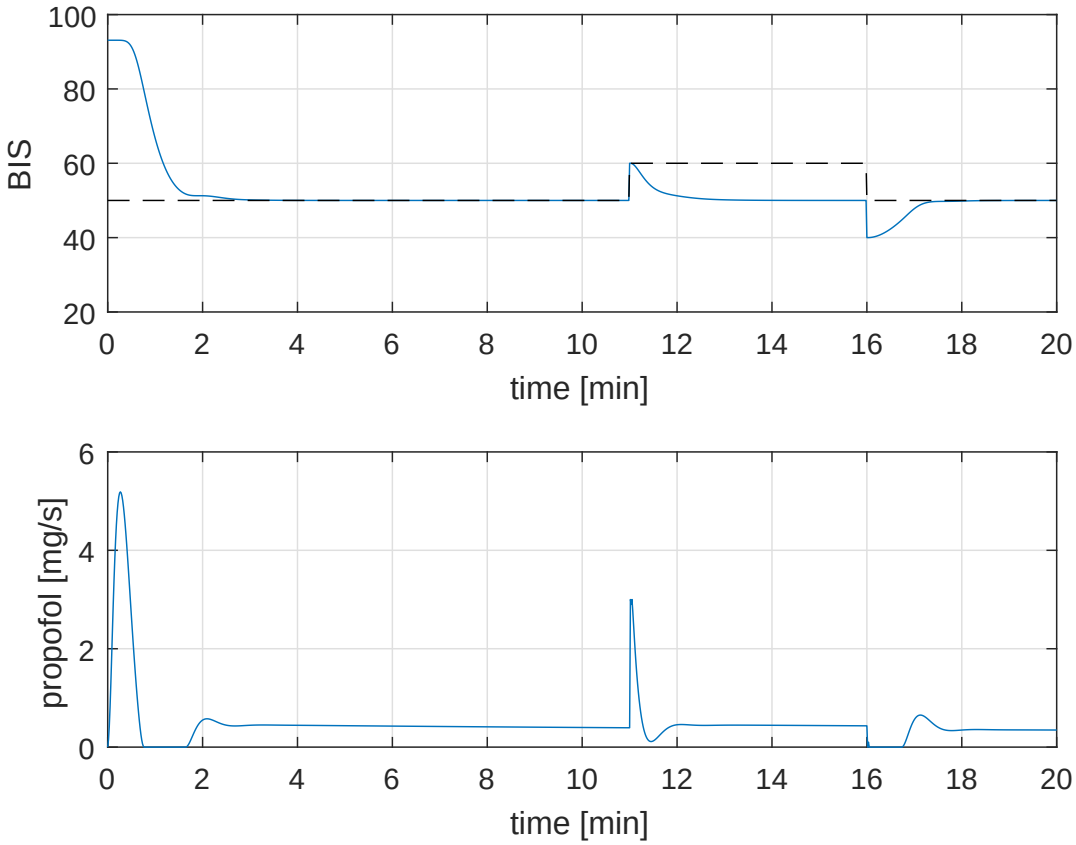

Figure 3.3: BIS signal and manipulated variable for the average patient in the SISO system.

- TT: observed time-to-target (in seconds) required for reaching the first time the target interval of $[45 \div 55]$ BIS values;
- BIS-NADIR: the lowest observed BIS value;
- ST10: settling time, defined as the time interval for the BIS to reach and steady within the BIS range between 45 and 55 (that is, the target value of 50 ± 5);
- ST20: the same of ST10 but it considers a BIS range of 40 and 60;
- US: undershoot, defined as the difference between the lower threshold of 45 and the minimum value of BIS below this threshold.

TT [min]	BIS-NADIR	ST20 [min]	ST10 [min]	US
1.37	50.00	1.18	1.37	0.00

Table 3.3: Set-point response for the average patient 13.

TTp [min]	BIS-NADIRp	TTn [min]	BIS-NADIRn
0.33	50.00	0.78	50.00

Table 3.4: Disturbance response for the average patient 13.

Regarding the load disturbance rejection task, only the TT and the BIS-NADIR indexes are meaningful and they are calculated separately for the positive (p) and for the negative (n) step signal. These indexes will also be used to make comparisons with other works. The satisfaction of the performance is confirmed by the indexes analysis, reported in table 3.3, where TT is equal to ST10, which means that the BIS signal does not exceed the 45 and 55 thresholds. Considering the disturbance rejection task, that is the compensation of possible noxious stimuli during the maintenance phase, it is possible to notice that the control action increases to compensate the first (positive) step in order to decrease the DoH of the patient and vice versa with the second (negative) step. The controller response for this task is much more aggressive compared to the set-point tracking one, because a fast rejection of the disturbances is required. The same performance indexes proposed for the set-point response are evaluated for each disturbance step; as shown in table 3.4 the indexes for the positive step are denoted with the letter 'p' and for the negative step with letter 'n', respectively. The settling times TTn and TTp are satisfactory for the clinical practice: the controller allows a fast disturbance rejection without excessive overshoot in the BIS level, as it is proven by BIS-NADIRp and BIS-NADIRn. TTn is higher than TTp because of the lower saturation limit of the pump. In fact, when a negative step disturbance occurs, the controller has to decrease the infusion in order to increase the DoH of the patient but the lower infusion limit is zero. Therefore, the BIS level increases naturally and this implies a higher settling time.

3.2.3 Robustness

A critical aspect to consider in the developed control is the robustness, that is the ability of the system to cope with variations of the model. In the theory of classical automatic controls, the work is developed with a dynamic system described in the form of a state or by its transfer function, known in a complete and accurate way, and an ad-hoc controller for that system is designed with different techniques. In practice this is not possible because the system is developed on a model that roughly describes the real system. The control that succeeds in solving this problem is said to be robust precisely because it guarantees the asymptotic stability for a set of systems and not only for just the nominal one. The problem of robustness in the application considered in this report is even more complex. In fact, there is an uncertainty of the model due to the fact that it is difficult to accurately consider and describe every aspect of the human body's response to drugs. In addition to this, there is the problem that the model must consider the intra-subject variability: each patient can react differently to propofol depending on their physical characteristics and their state of health. The developed controller must ensure correct functioning in each case, avoiding the onset of problems that could endanger the patient's health. If, for example, the controller generates a correct control action for one patient, but is too high for another patient, dangerous undershoot may occur with respect to the established reference.

The controller robustness is therefore a fundamental characteristic for the automatic control of DoH and it has to guarantee satisfactory performance despite of the inter- and intra-patient variability. The same tests performed on the average patient 13 have been performed on the entire population of table 1.1 in order to validate the robustness to inter-patient variability. In this test the average Hill function is considered and the hypothesis of perfect knowledge of the process model is applied ($\tilde{P} = P$). The process output and the control action for the induction phase are shown in figure 3.4. As can be appreciated from the figure, the control actions are very similar to each other, that is, despite the variability of the model, the controller generates comparable actions. Also the outgoing BIS signals

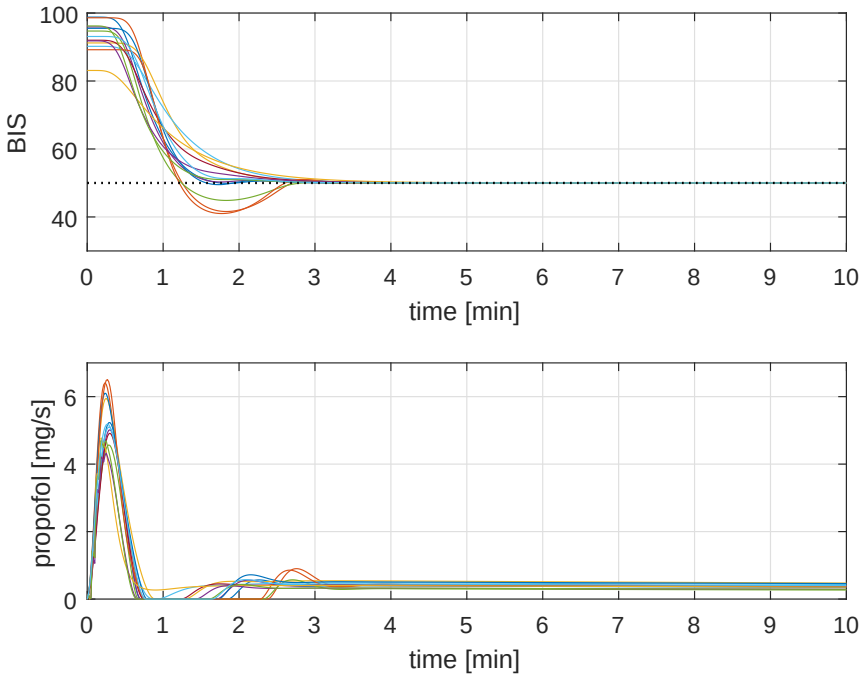

Figure 3.4: BIS level and control action in the induction phase for each patient.

are very similar: all patients enter the BIS range of [60-40] in the established time (about 100 [s]) and all stabilize at the established reference in comparable times. The transient during which the BIS is brought to the regimen turns out to be practically identical for every patient: some differences in terms of oscillations are noticed, as some subjects tend to have a more oscillating behavior, but correct as included in the range [60 -40].
It is possible to say that clinical specifications are always fulfilled despite the inter-patient variability, as can be verified by analyzing the performance indexes in table 3.5.

The control system robustness to inter-patient variability is verified also for the disturbance rejection case. In figure 3.5 the response of the disturbance is shown for each patient and the corresponding indexes are shown in table 3.6. Settling times and BIS undershoots are satisfactory with respect to the clinical practice.
The same tests performed on the set of patients reported in table 1.1 have then been executed on 500 patients generated by applying a Monte Carlo method in order to further validate the controller robustness to the inter-patient variability, as done in [36]. The

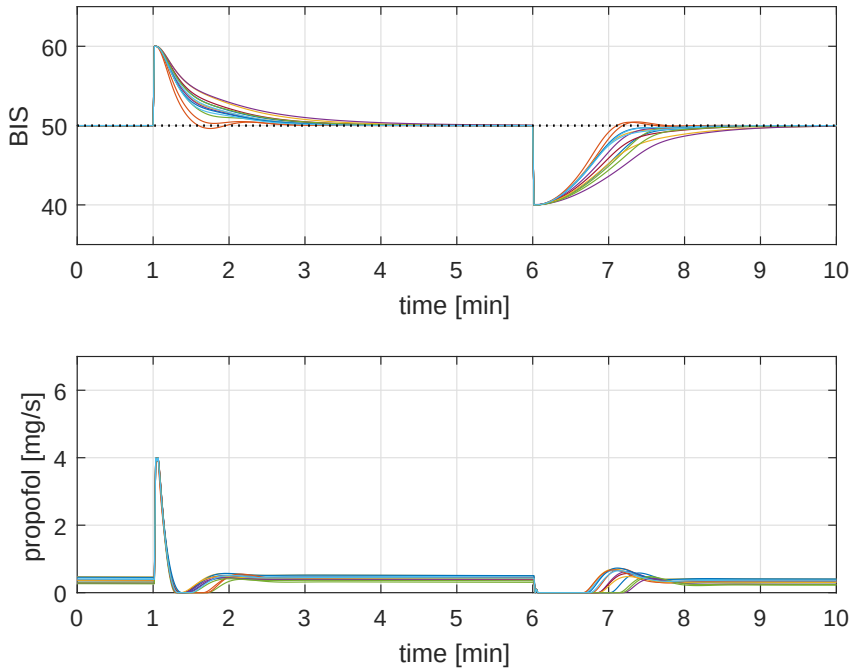

Figure 3.5: BIS level and control action in the maintenance phase for each patient.

Patient	TT [min]	BIS-NADIR	ST20 [min]	ST10 [min]	US
1	1.27	49.89	1.08	1.27	0.00
2	1.15	41.60	1.05	2.33	3.40
3	1.75	50.00	1.40	1.75	0.00
4	1.25	50.00	1.07	1.25	0.00
5	1.07	44.86	0.95	1.95	0.14
6	1.90	50.00	1.50	1.90	0.00
7	1.68	50.00	1.27	1.68	0.00
8	1.27	49.51	1.12	1.27	0.00
9	1.12	41.01	1.05	2.28	3.99
10	1.92	50.00	1.38	1.92	0.00
11	1.35	50.00	1.03	1.35	0.00
12	1.20	50.00	0.98	1.20	0.00
13	1.37	50.00	1.18	1.37	0.00
mean	1.41	48.22	1.16	1.66	0.58
std.dev	0.30	3.38	0.17	0.40	1.39
max	1.92	50.00	1.50	2.33	3.99
min	1.07	41.01	0.95	1.20	0.00

Table 3.5: Performance indexes for the set-point tracking of each patient.

Patient	TTp [min]	BIS-NADIRp	TTn [min]	BIS-NADIRn
1	0.40	50.00	0.98	49.99
2	0.28	50.00	0.75	50.46
3	0.37	50.00	0.77	50.00
4	0.37	50.00	0.85	50.00
5	0.33	50.00	1.02	50.00
6	0.38	50.00	0.77	49.99
7	0.42	50.01	0.92	49.98
8	0.33	50.00	0.78	50.00
9	0.27	49.63	0.70	50.42
10	0.50	50.02	0.98	49.93
11	0.50	50.05	1.22	49.93
12	0.40	50.01	1.08	49.99
13	0.33	50.00	0.78	50.00
mean	0.38	49.98	0.89	50.05
std.dev	0.07	0.10	0.16	0.17
max	0.50	50.05	1.22	50.46
min	0.27	49.63	0.70	49.93

Table 3.6: Performance indexes for the disturbance rejection of each patient.

PKPD models are generated by considering the average values of the model parameters. The patient models are randomly calculated by considering a uniform distribution of the age between 18 and 70, of the height between 150 $[cm]$ and 190 $[cm]$, and of the weight between 50 $[kg]$ and 100 $[kg]$. Then, the distribution of the values for the Hill function parameters have been taken from [7]. As in previous case, P is fixed equal to $\tilde{P}$ and $\tilde{H}$ is chosen as the average Hill equation. The results for the induction phase are shown in figure 3.6, while those related to the maintenance phase are shown in figure 3.7. The corresponding indexes are shown in tables 3.7 and 3.8. We note that two patients have an undershoot that exceeds the lower limit of 40. The problem is not relevant, as the excessive overshoot is minimal, reaching a BIS of 38 and 39 respectively.

The simulated results show that the control system is robust with respect to the inter-patient variability as all the clinical specifications are always fulfilled. In the previous test a perfect knowledge of the patient model has been assumed, because the objective was to test the robustness of the controller over a wide population. We also want to test

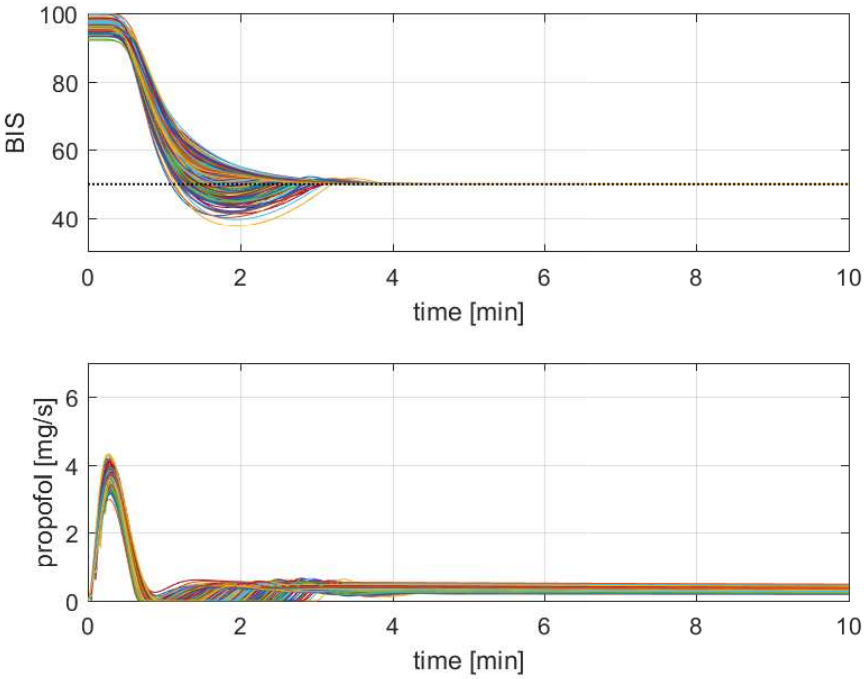

Figure 3.6: Set-point step responses by using MCM for inter-patient variability.

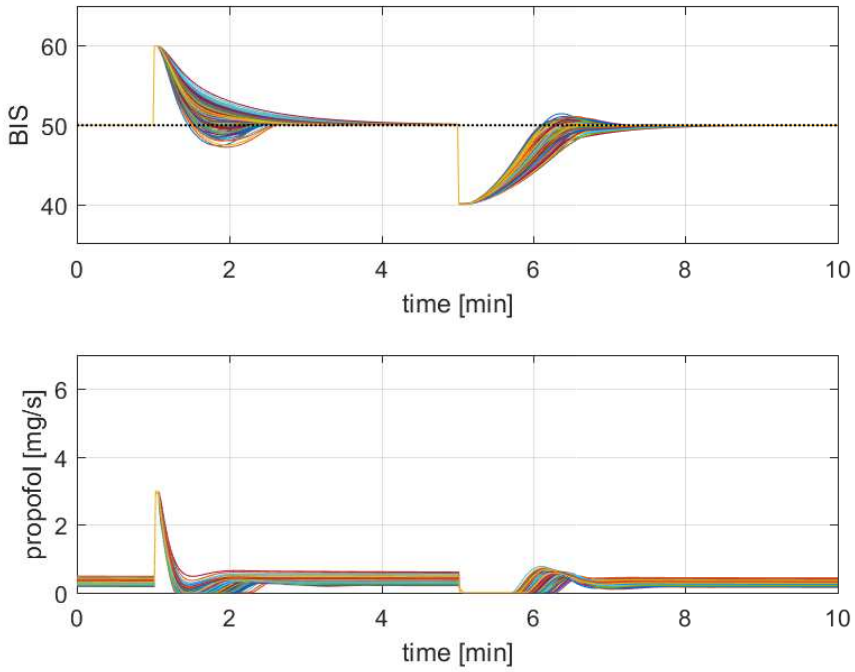

Figure 3.7: Load disturbance responses by using MCM for inter-patient variability.

	TT [min]	BIS NADIR	ST10 [min]	ST20 [min]	US
mean	1.46	49.16	1.18	1.51	0.12
std dev	0.21	1.91	0.13	0.29	0.66
min	0.98	37.64	0.88	1.08	0.00
max	2.03	50.00	2.43	2.87	7.36

Table 3.7: Performance indexes for the set-point tracking task with the MCM for inter-patient variability.

	TTp	BIS-NADIRp	TTn	BIS-NADIRn
mean	0.37	49.91	0.89	50.21
std.dev	0.05	0.34	0.08	0.26
max	0.25	47.24	0.70	50.00
min	0.60	50.00	1.13	51.45

Table 3.8: Performance indexes for the load disturbance rejection task with the MCM for inter-patient variability.

the robustness of the controller against the mismatches of the linear part of the model, that is, the intra-patient variability. To this end, we consider the statistical distribution of the PKPD model parameters reported in section 1.3.1. In particular, for each patient of table 1.1, $\tilde{P}$ is calculated based on the average parameters values used in section 1.3.1 and P is generated by applying another MCM on the parameters statistical distribution. For each patient, a set of 500 models has been generated based on the statistical properties of the model shown in [19]. For the sake of readability, only the performance indexes related to the average patient 13 are given below. The responses of the average patient for the induction phase are shown in figure 3.8 and the corresponding performance indexes are shown in table 3.9. Despite the intra-patient variability, the set-point response is always satisfactory and the clinical specifications are always fulfilled. It is well known that when the model is very different from the real process, the performance of a predictive controller based on that model is heavily influenced and achieving a good level of robustness could be very difficult. For this reason it is possible to confirm the intra-patient robustness for all the other patients, see figure 3.10, even if for patient 2 and patient 9 in some cases the BIS goes under the level of 40. The results for the maintenance phase of average patient 13 are shown in figure 3.9 and the performance indexes are reported in table 3.10, while the

TT [min]	BIS-NADIR	ST20 [min]	ST10 [min]	US
1.40	49.57	1.17	1.39	0.00
0.11	0.88	0.05	0.12	0.04
1.17	44.10	1.02	1.15	0.00
1.90	50.21	1.40	2.17	0.90

Table 3.9: Performance indexes for the set-point tracking task with the MCM for intra-patient variability (average patient 13).

TTp [min]	BIS-NADIRp	TTn [min]	BIS-NADIRn
0.39	49.98	0.78	50.04
0.02	0.07	0.04	0.05
0.33	49.74	0.67	49.93
0.45	50.20	0.90	50.31

Table 3.10: Performance indexes for the load disturbance rejection task with the MCM for intra-patient variability (average patient 13).

results for all the patients are shown in figure 3.11. Also in these cases the intra-patient robustness is verified.

From this analysis the developed system turns out to be robust and able to cope to the variability of patient models. The excellent results obtained therefore push then to continue the development of the automatic control system for anesthesia.

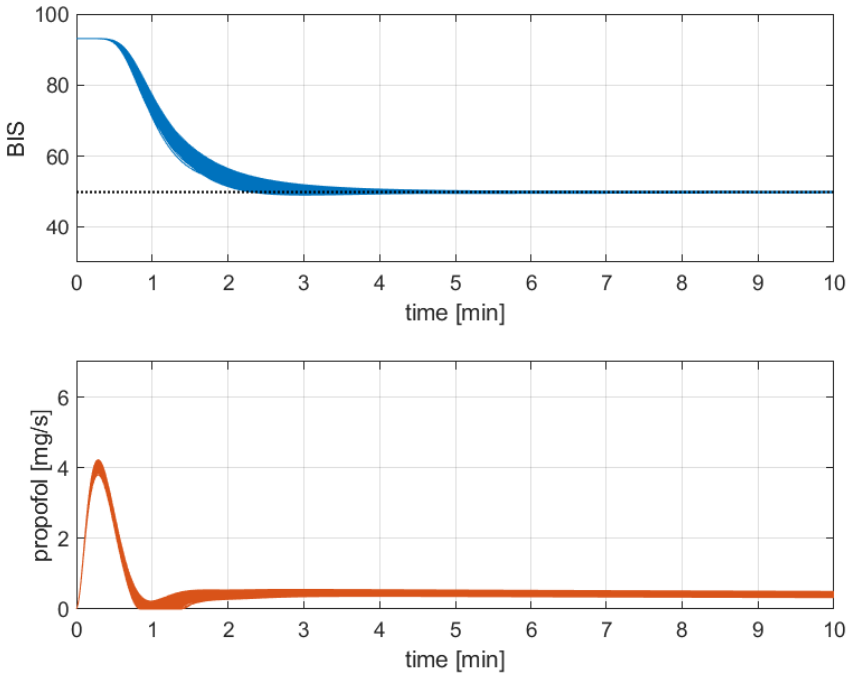

Figure 3.8: Set-point step responses for intra-patient robustness (average patient 13).

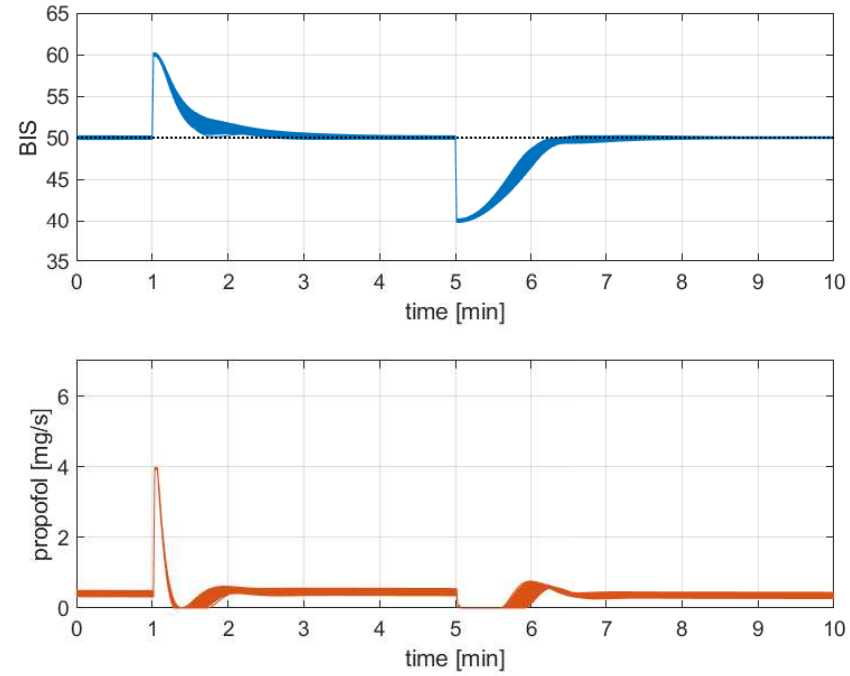

Figure 3.9: Load disturbance responses for intra-patient robustness (average patient 13).

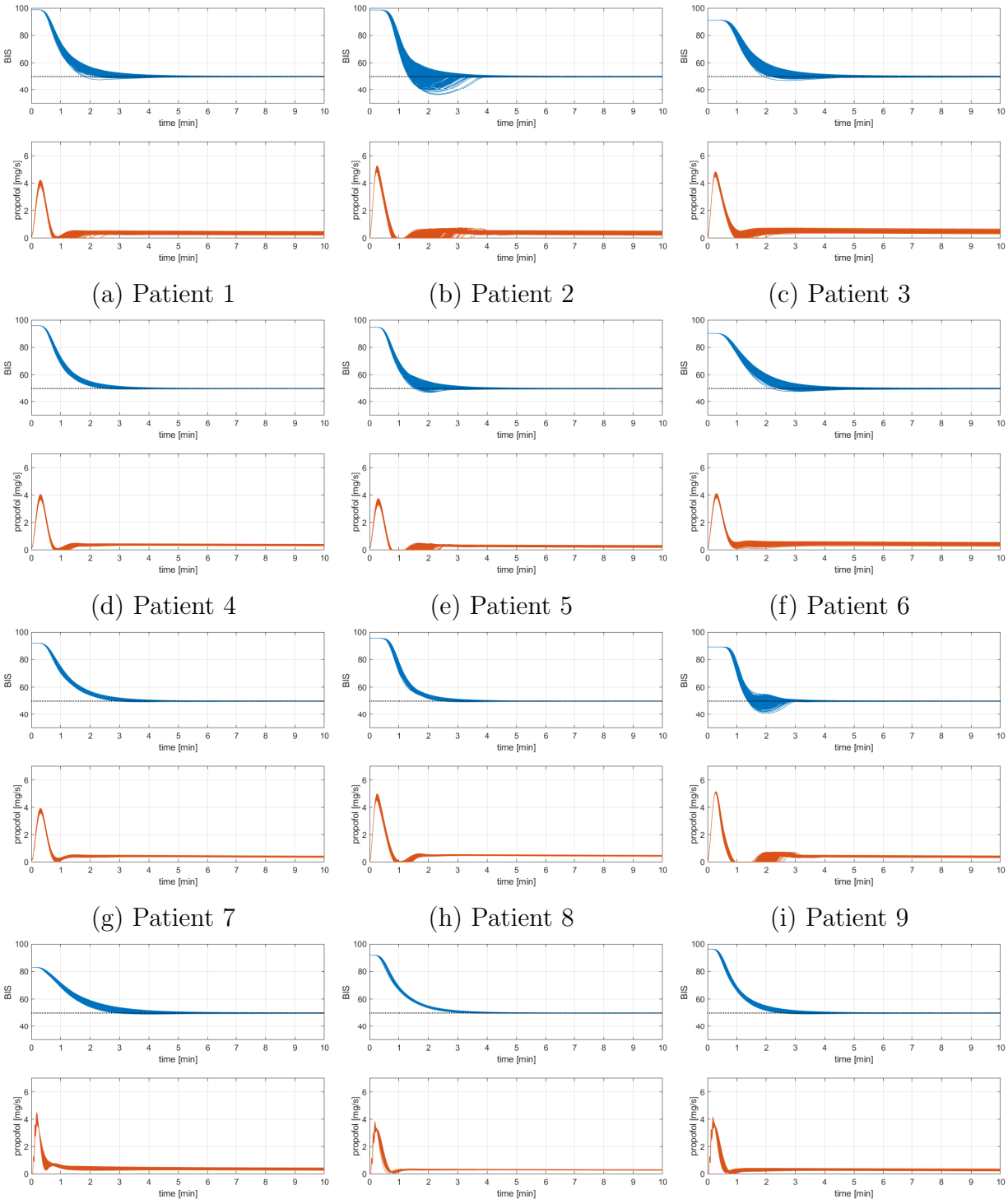

(a) Patient 1 (b) Patient 2 (c) Patient 3

(d) Patient 4 (e) Patient 5 (f) Patient 6

(g) Patient 7 (h) Patient 8 (i) Patient 9

(j) Patient 10 (k) Patient 11 (l) Patient 12

Figure 3.10: MCM results for the set-point step response for all patients.

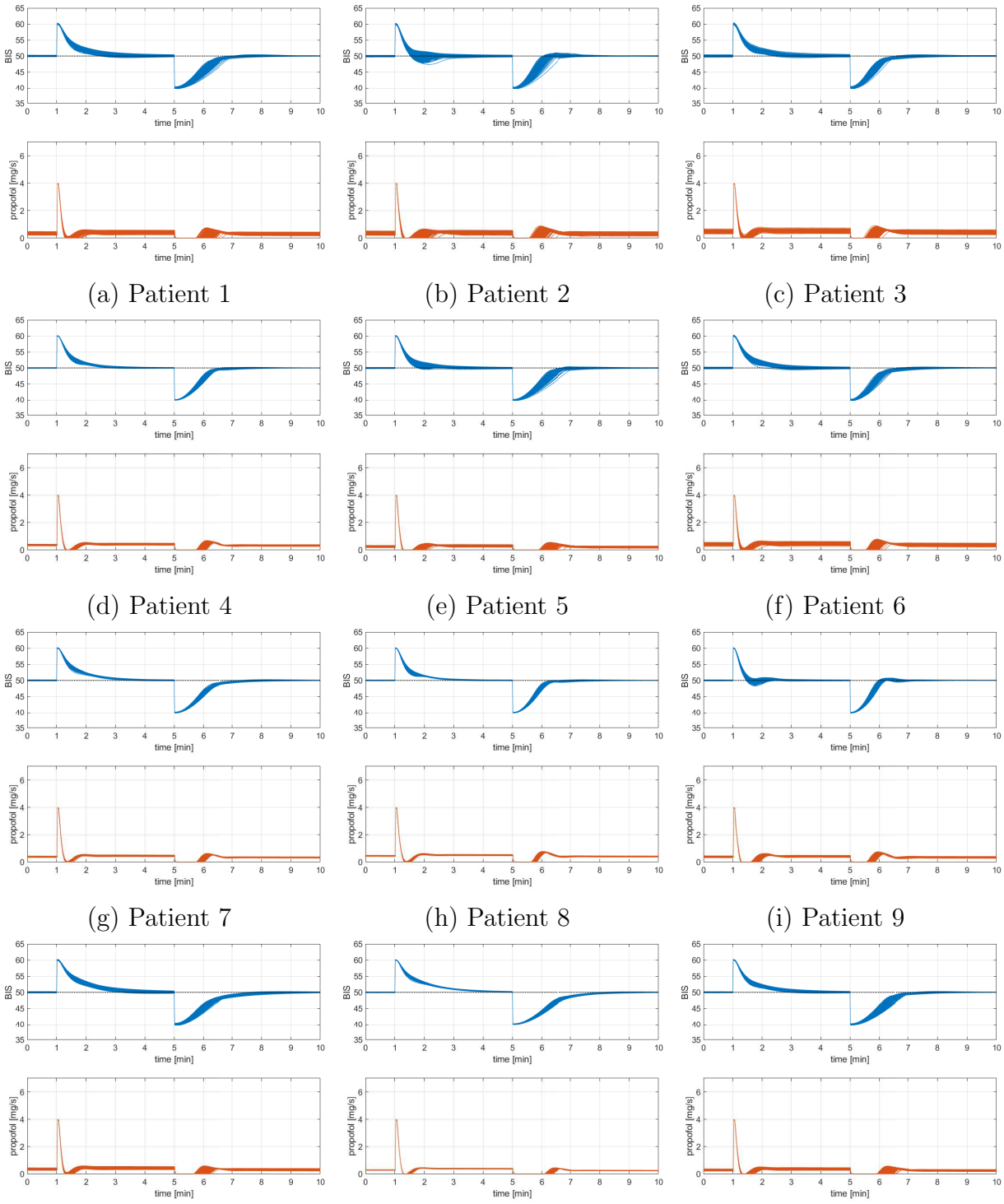

(a) Patient 1 (b) Patient 2 (c) Patient 3

(d) Patient 4 (e) Patient 5 (f) Patient 6

(g) Patient 7 (h) Patient 8 (i) Patient 9

(j) Patient 10 (k) Patient 11 (l) Patient 12

Figure 3.11: MCM results for the load disturbance response for all patients.

3.3 Comparison with other control systems

After testing the usability of the SISO control system developed for the propofol only infusion, it is now possible to perform comparisons on performance with other system. The first comparison will be with a standard PI controller, which includes an anti-windup method and it uses two different set of parameters, one used for the induction phase and the other for the maintenance phase. In figure 3.13 it is possible to observe the implementation of the system for the control of the hypnotic propofol drug alone (SISO system). The PI has the following formulation:

$$C(s) = K_p \left(1 + T_i \frac{1}{s}\right) \tag{3.8}$$

where K_p is the proportional gain and T_i is the integral time constant. As already mentioned, two different set of parameters will be used and the tuning is obtained in both cases with the GA as it cannot be performed with the calibration laws in the literature. This is because the process is complex and nonlinear and linearizing and approximating with a simpler model would result in the loss of fundamental information about the dynamics of the system. Table 3.11 shows the tuned parameter used for the induction phase and the maintenance phase. Figure 3.12 shows the comparison between the response of the GPC and the PI with the average 13 patient. As it is possible to notice, the GPC presents a faster and less oscillating trend but the PI has a smoother control action. It is worst also the positive disturbance rejection, while for the negative is more or less the same. This is also confirmed by the IAE calculated on the results: 7824 for the PI and 3922 for the GPC. The better performance of the GPC are attributable to the fact that the process is slow and since the GPC knows the model it can act in advance on future errors, while the

	Induction	**Maintenance**
K_p	0.0294	0.0605
T_i	400.855	409.049

Table 3.11: Tuning parameters of the PI controller.

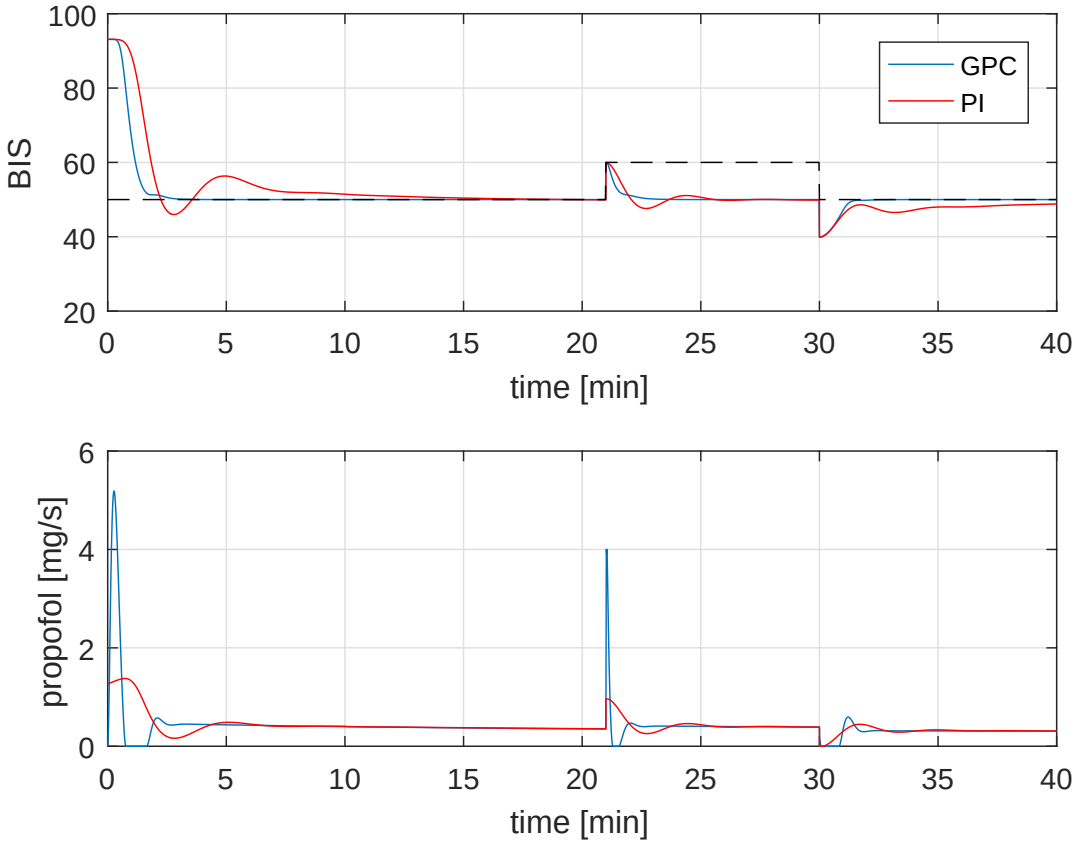

Figure 3.12: Comparison between the response of the GPC and PI controllers with the average patient 13.

PI reacts later, only when it detects the error. It is worth pointing out that during the simulation the GPC controller is using the same amount of drugs as the PI controller.

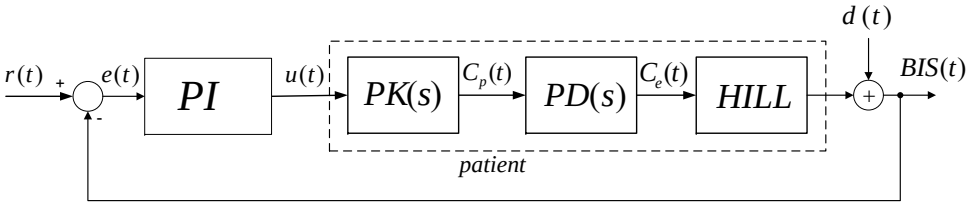

Figure 3.13: Implementation of the SISO control scheme with standard PI for the propofol regulation.

To test the behavior of the controller under real condition it is possible to make a simulation with the disturbance profiles used in [38], which are reported in figure 3.14 and figure 3.15. In [38] it is implemented a combined strategy of MPC and least squares online parameter estimation for the control of the hypnotic depth. The system is composed by a conventional online MPC with a Kalman filter implemented to obtain an estimate of the states plus an online estimator added to the closed control loop for the estimation of the PD parameter C_{50} during the course of surgery. The block diagram of this system is reported in figure 3.16.

It is only possible to make a visual comparison with the results obtained with the MPC because no performance indicator is calculated in the article, only the BIS trends are

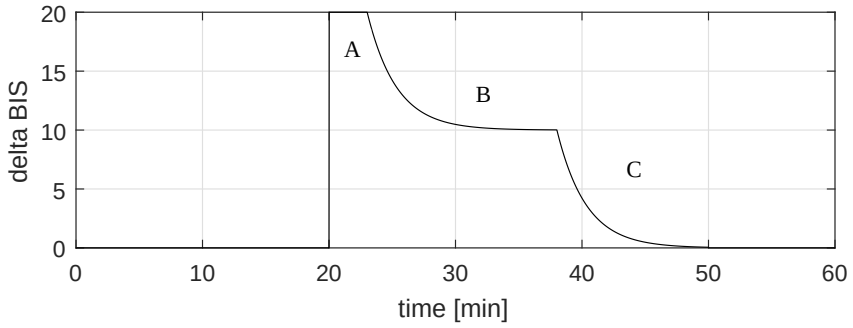

Figure 3.14: Disturbance profile:(A) arousal reflex due to the first surgical incision; (B) offset slowly decreases but settles at on onset of 10% due to continuous normal surgical stimulations; (C) withdrawal of stimulations during skin-closing.

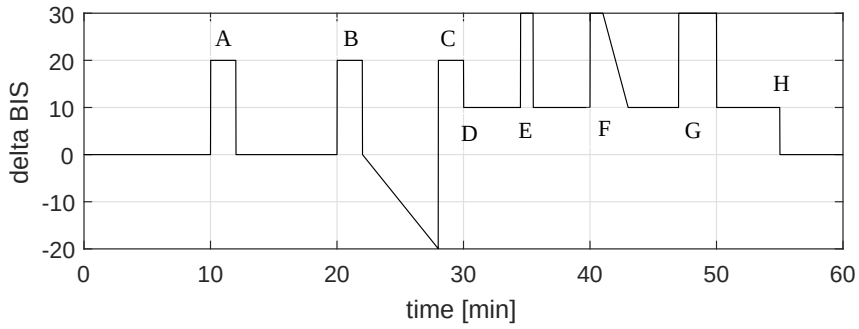

Figure 3.15: Disturbance profile: (A) laryngoscopy/intubation; (B) surgical incision followed by no surgical stimulation; (C) abrupt stimulus after a period of low stimulation; (D) onset of a continuous normal surgical stimulation; (E-G) stimulate short-lasting, larger stimulations; (H) withdrawal of stimulations during closing.

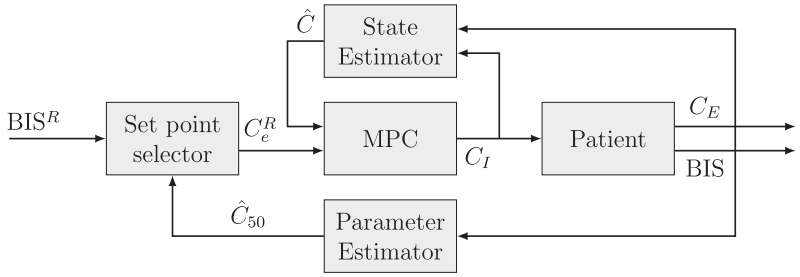

Figure 3.16: Control system used in [38].

presented. The images in the article are therefore reported, together with the response of the GPC controller: at the top of figure 3.17 there is the response of the MPC in [38], with the BIS trend in dash-dotted line, while at the bottom there are the BIS trend and the control signal of the 13 patients of table 1.1, obtained with the GPC. Comparing the results it is possible to observe that even in this case the GPC provides a faster disturbance rejection: this consists in a better response for the first disturbance profile, as the BIS stays for more time at the desired level. In fact with the GPC the BIS begins to reach the reference immediately after the step disturbance (A) of figure 3.14, while the MPC needs more time to react. The same happens for the last part (C) of the disturbance profile, resulting in having less undershoot for the GPC case.

Looking at figure 3.18, that reports the system response at disturbances profile in figure

3.14, it is possible to notice that the fastness of the GPC causes a positive peak that makes the BIS reach the 80 unit. That is because the step of +40 BIS unit in point C of figure 3.15: for the MPC it does not produce a +40 increment on the reference signal because in that moment the MPC is still compensating for the previous negative step and the BIS is under the reference. So, in this case, it is possible to say that the controller slowness gives advantages.

Besides of this unlucky combination we can say that the GPC performs better than the MPC of [38], because normally it has a faster action, and in case of need it can be slowed down (by incrementing the value of λ in equation 2.7) to achieve a similar behaviour of the MPC. In both cases it is not possible to make observation on the control signals because they are not reported in the article.

Having achieved good results in comparison with other controllers, it is now possible to proceed further, introducing remifentanil infusions into the system.

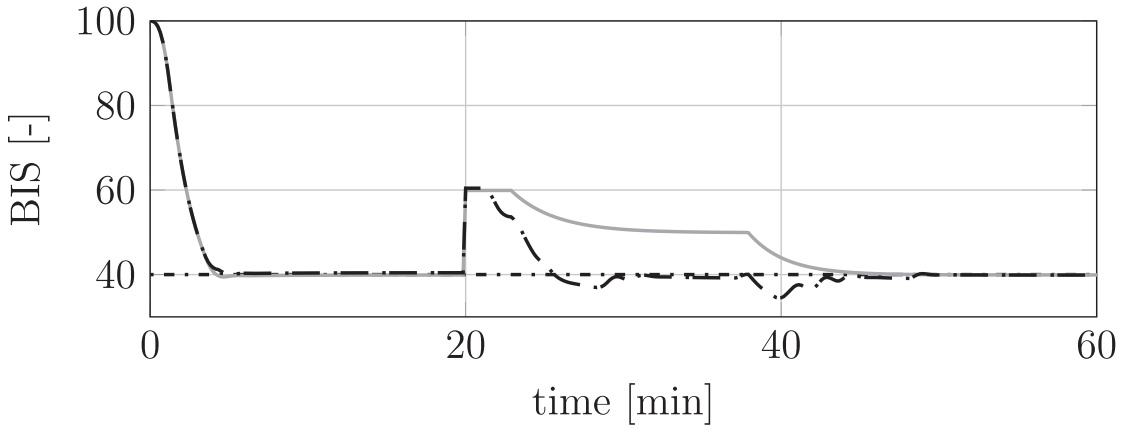

(a) MPC

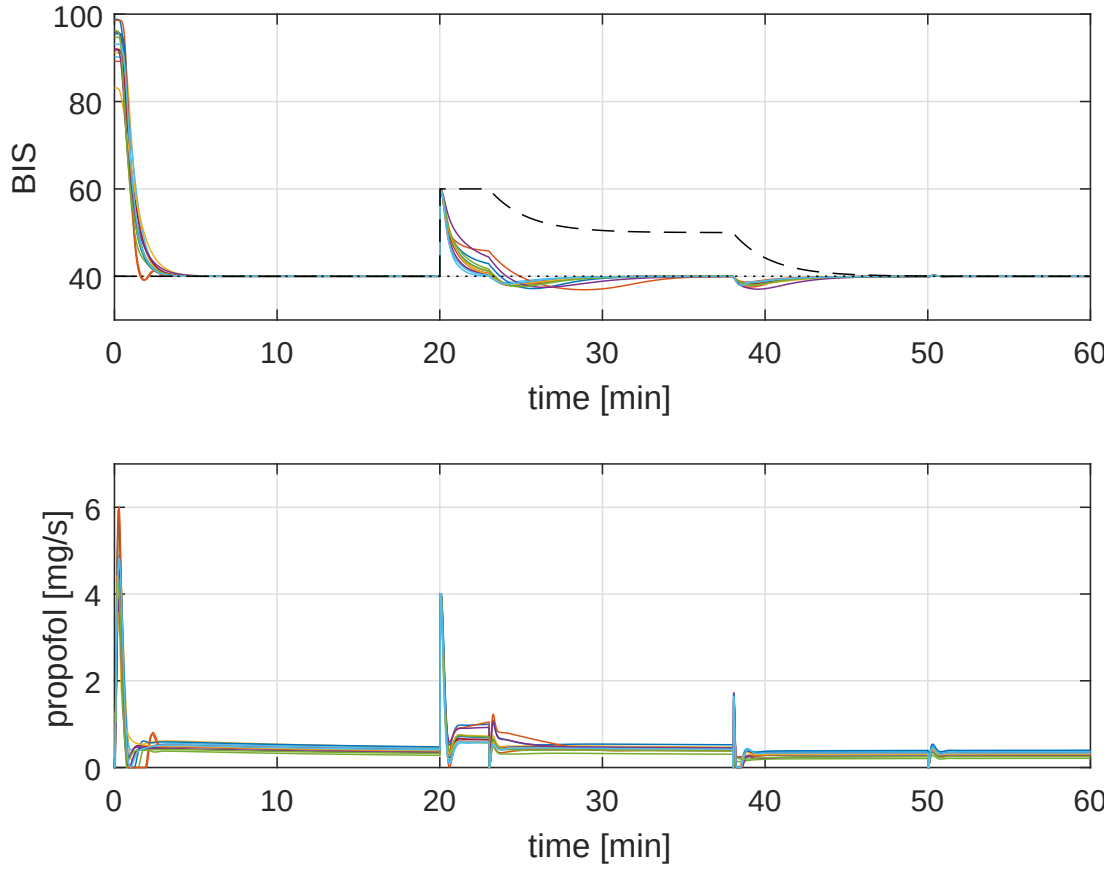

(b) GPC

Figure 3.17: BIS responses for disturbances profile in figure 3.14.

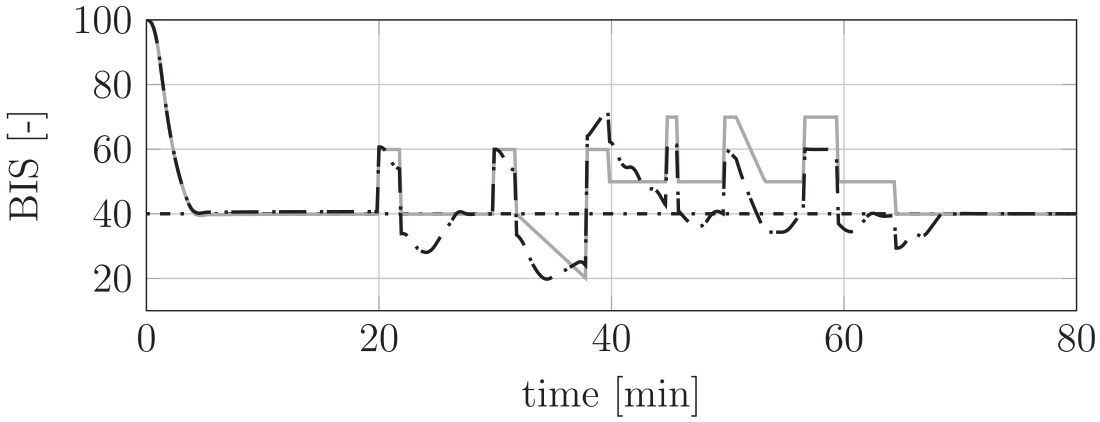

(a) MPC

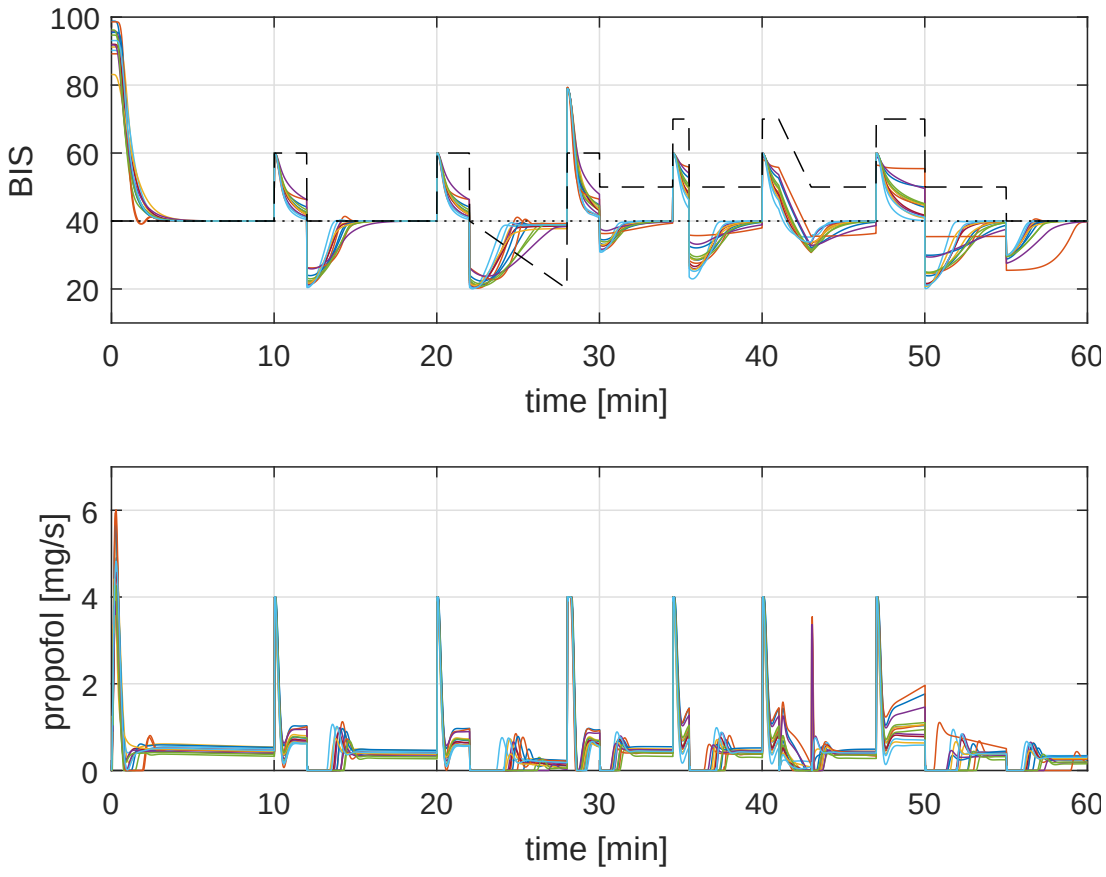

(b) GPC

Figure 3.18: BIS responses for disturbances profile in figure 3.15.

Chapter 4

Complete system

In the previous chapter the work was focused on obtaining an efficient and robust controller for the infusion of the anesthetic drug propofol. This chapter presents the control scheme capable to set the infusion rate of the anesthetic and analgesic drugs, i.e. propofol and remifentanil, using the BIS signal as controlled variable (MISO system). This is possible because the remifentanil has an influence on the effect of the propofol which means that variations on the remifentanil infusion rate will provoke variation on the BIS signal. The idea is to exploit the control scheme previously developed for the propofol and set the remifentanil infusion rate with a gain over the propofol infusion, as it is usually done by the anesthesiologist. So by taking into account the synergistic effect between the two drugs, the controller must compute the correct propofol infusion profile, then the remifentanil the dose is selected by multiplying the infusion rate by a gain previously established.
The development of this system allows the automatic administration of anesthesia, as foreseen by the objective of the thesis.

4.1 Control requirements

The control structure of the MISO system provides for the automatic regulation of the combined infusion of propofol and remifentanil drugs, using the BIS signal as feedback for

the regulation of propofol. The goal is therefore to create a controller that brings the level of hypnosis of the patient to a desired value in a time interval suitable for the application. The medical specifications that the control system must meet are the same as those presented for the propofol-only regulation system. They have been provided by the Spedali Civili di Brescia and provide a reference BIS of 50 to be reached in less than 5 $[min]$ (preferably in a shorter time, as about 120 $[s]$), limited undershoot and the general consideration of minimizing the drugs administration to obtain the desired DoH.

The system must also be robust enough to cope with the variability of the model, due to the different characteristics and health status of the patients. This property is fundamental to the particular application considered, in order to avoid risks to the health of patients.

An additional specification to be considered concerns the limits to the generated control action, which are the infusion rate bounds of a standard pump (Graseby 3400, Smiths Medical, London, UK). The lower saturation corresponds to the zero infusion for both drugs while the maximum rate is 6.67 $[mg/s]$ for propofol (Diprivan 20 $[mg/ml]$) and 16.67 $[\mu g/s]$ for remifentanil (Ultiva 50 $[\mu g/s]$) [39].

Summarizing the control specifications to be considered are those described in the table 4.1.

Set-point reference	50
Undershoot	10 $\%_{FS}$
Settling time	120 $[s]$
Propofol upper sat.	6.67 $[mg/s]$
Propofol lower sat.	0.0 $[mg/s]$
Remifentanil upper sat.	16.67 $[\mu g/s]$
Remifentanil lower sat.	0.0 $[\mu g/s]$

Table 4.1: Specifications of the MISO control system.

4.2 Control scheme

Unlike the system presented in the previous chapter, the control here developed must consider the drugs synergistic effect in order to correctly infuse anesthesia. When the

propofol is administrated together with the remifentanil, its effects over the DoH are amplified as modeled in equation 1.26. Figure 4.1 represents the implemented control scheme, which is based on the one used in section 3.2. This control scheme tries to emulate the behaviour of the anesthesiologist who sets the remifentanil infusion rate with a gain over the propofol rate and then his/her work is to monitor and regulate the propofol infusions in order to obtain the desired BIS level. The value of the ratio K depends on many factors, first of all the type of surgery, and it is decided by the anesthesiologist thanks to his/her experience. Usual values ranges between 0.5 and 15 with the propofol measured in $[mg/s]$ and the remifentanil in $[\mu g/s]$.
In the same way as in section 3.2, the blocks $\tilde{P}_{prop}$ and $\tilde{P}_{remif}$ are considered equals, which means that a perfect knowledge of the linear parts is assumed. Otherwise, the parameters of the non-linear Hill function are unknown and for the $\tilde{H}^{-1}$ block the average parameters found in the literature are used. More precisely the parameters are the one used in [7] and [40] and their values are 87.5, 4.92 $[\mu g/ml]$, 12.5 $[ng/ml]$, 2.69, 1.5 respectively for E_{max}, C_{50prop}, $C_{50remif}$, γ, β. The parameter E_0 can be measured and the correct value will be used for each patient.
F_d is a low pass filter, in the form:

$$F_d(s) = \frac{1}{T_d s + 1} \tag{4.1}$$

In the design of the control system it was necessary to take into consideration the following aspects:

1. the inverse Hill function block $\tilde{H}^{-1}$ must take into account also the contribute of the remifentanil;

2. the contribute of the remifentanil should also be considered for the calculation of the reference signal;

3. the anesthesiologists use different value of the ratio between propofol and remifentanil

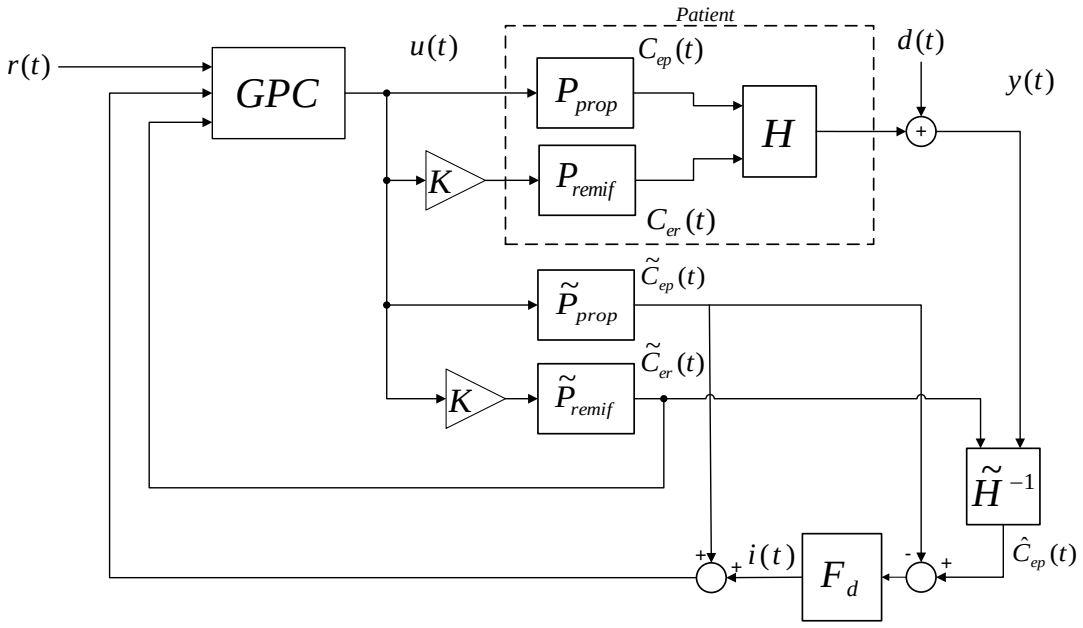

Figure 4.1: The MISO control scheme for the automatic regulation of propofol and remifentanil during anesthesia.

infusions rate, so we have to do an optimization for each value of the ratio.

For the first point, the equation (1.26) needs to be reversed, in order to obtain something in the form of: $U_{prop}(t) = f(BIS(t), U_{remif}(t))$. To achieve that, it is possible to modify (1.26) in the form of a third degree equation:

$$U_p^3 + bU_p^2 + cU_p + d = 0 \tag{4.2}$$

with:

$$b = 3U_r - \left(\frac{E_0 - BIS}{E_{max} - E_0 + BIS}\right)^{1/\gamma}$$
$$c = 3U_r^2 - 2U_r\left(\frac{E_0 - BIS}{E_{max} - E_0 + BIS}\right)^{1/\gamma} + \beta U_r\left(\frac{E_0 - BIS}{E_{max} - E_0 + BIS}\right)^{1/\gamma}$$
$$d = U_r^3 - U_r^2\left(\frac{E_0 - BIS}{E_{max} - E_0 + BIS}\right)^{1/\gamma}$$

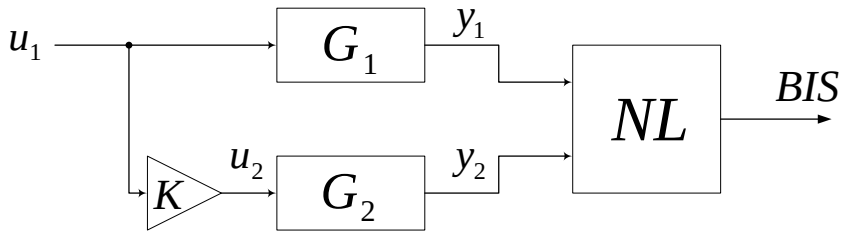

Figure 4.2: Simplified scheme for the patient model.

where U_p and U_r are propofol and remifentanil effect-site concentrations normalized with respect to the concentration that produces half of the maximal effect:

$$U_{prop}(t) = \frac{C_{e,p}(t)}{C_{e_{50},p}}, \quad U_{remif}(t) = \frac{C_{e,r}(t)}{C_{e_{50},r}}, \tag{4.3}$$

In this way, knowing the actual BIS and the estimated remifentanil effect site concentration $\tilde{C}_{e,r}(t)$ it is possible to solve the equation and calculate $\hat{C}_{e,r}(t)$.

The equation (4.2) cannot be directly used for the calculation of the reference signal, because it depends also on the U_{remif}. As it is possible to see also from the simplified representation in figure 4.2, the remifentanil infusion is linked at the propofol infusion by means of a gain, so it is therefore possible to express U_{remif} in function of U_{prop}.

$$y_1 = G_1 u_1 \qquad\qquad y_2 = G_2 u_2 = G_2 K u_1$$

From here it is possible to obtain:

$$y_2 = G_1^{-1} G_2 K y_1 \tag{4.4}$$

Which can be written in the form of difference equation:

$$y_2(k) = b_0 y_1(k) + b_1 y_1(k-1) + ... + b_7 y_1(k-7) - a_1 y_2(k-1) - a_2 y_2(k-2) - ... - a_7 y_2(k-7) \tag{4.5}$$

At this point it is possible to substitute U_{remif} in the equation (4.2) with $U_{remif}(U_{prop})$ from equation (4.5) obtaining an equation in which the propofol concentration depends only by the desired BIS level. Thus it is possible to calculate an optimal reference signal for the propofol infusions, keeping in mind that this value can undergo slight variations at every sample time because the relation between y_1 and y_2 is not fixed and depends on the past values of y_1 and y_2.

4.2.1 Tuning of the parameters

Observing figure 4.1 it seems that there is one less parameter to calibrate than the control scheme used in chapter 3.2 as the F_r block has disappeared. This is because the use of the filter on the reference cannot handle the aggressiveness of the controller with the two drugs infused, and for this scheme we decided to handle the set-point following and disturbance rejection tasks in a different manner. Firstly the controller will be tuned to obtain an optimal set-point response, then another tuning procedure will be made maintaining N and N_u from the found parameters and searching λ and T_d for the best disturbance rejection. In this case, in order to change λ and T_d online we need to include in the scheme two different low pass filters with a bumpless strategy to have smooth transitions. In figure 4.3 it is possible to see how the bumpless strategy is implemented: when one filter is working the other is in *following mode* which means that its output is modified to be the same as the actual output. Then, when the change occurs, the role are reversed.

To change from one set of parameters to another, we decided to activate the switch $S1$ after 300 $[s]$ from the set-point change. This is because after that period the induction phase should be considered finished and the maintenance phase begins. Is is important to mention that λ and T_d are the only parameters that can be changed online, as N and N_u establish the dimension of the matrixes in section 2.1 and the only possibility to have different N and N_u is to have two different controllers.

To summarize, the tuning consist in the research of six parameters for each value of

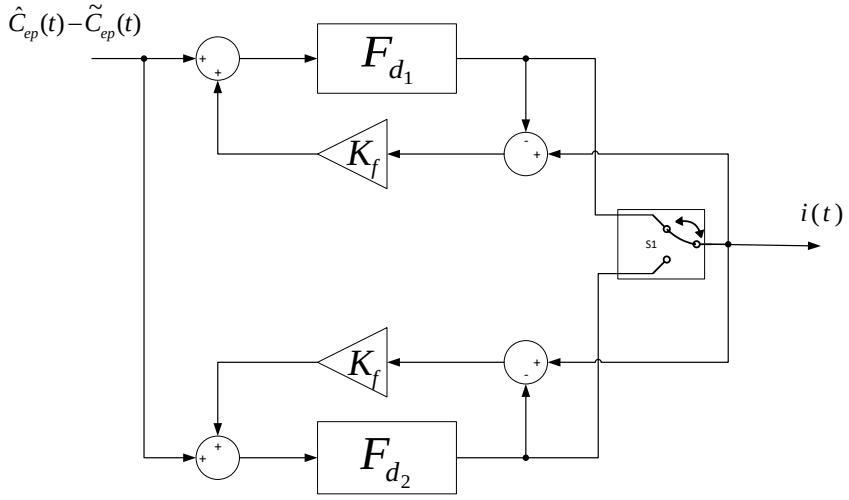

Figure 4.3: Detail of block F_d of figure 4.1.

the ratio K. As already mentioned above, the control system turns out to be MISO and non-linear and therefore it is necessary to use GA to derive the optimal set of tuning parameters. They were presented in section 2.2 and allow the determination of system parameters through subsequent simulations and analysis of the results obtained with the minimization of a cost function. The ratio value is not fixed and it ranges from 0.5 to 15 [1]. As starting point we decided to obtain the optimal set of parameter for 16 different values of K. The results are reported in table 4.2. With the table it is possible to use the control system only with the ratio of remifentanil and propofol reported in the first column, but not for values between them, like, for example, $K = 1.5$. To bypass this problem we have analyzed the table looking for trends in the parameter values and it turns out that for λ, T_{d1} and T_{d2} it is possible to interpolate the data with a first degree equation: in figure 4.4 are reported the values of the parameters together with the straight lines obtained with

[1] data provided by the Spedali Civili di Brescia.

K	**N**	$\mathbf{N_u}$	λ_1	$\mathbf{T_{d1}}$	λ_2	$\mathbf{T_{d2}}$
0,5	45	33	32	51	5	21
1	43	21	45	62	5	22
2	36	34	10	96	3	23
3	40	30	15	77	4	22
4	46	41	20	51	2	41
5	45	34	12	75	3	47
6	42	35	10	75	3	48
7	40	20	11	79	2	41
8	41	37	17	108	6	54
9	38	33	9	119	4	56
10	43	22	10	139	5	66
11	36	10	8	108	4	83
12	38	16	9	115	4	80
13	36	17	8	151	5	91
14	37	16	3	172	3	102
15	39	32	19	178	2	108

Table 4.2: Tuning parameters for different values of K.

interpolation. For the other parameter N, N_u, λ_2 we chose to use the average values:

$$N = 40$$

$$N_u = 31$$

$$\lambda_1 = 24.9572 - 1.3387 * K$$

$$T_{d1} = 45.6747 + 7.678 * K$$

$$\lambda_2 = 4$$

$$T_{d2} = 11.2321 + 6.019 * K$$

To verify the effectiveness of this strategy, the maximum IAE of the patients of table 1.2 was calculated for each K value, both with the parameters obtained with GA and with the interpolation. The average values of IAE reported in table 4.3, result very similar, so it is possible to confirm that the parameters found with the interpolation can be used.

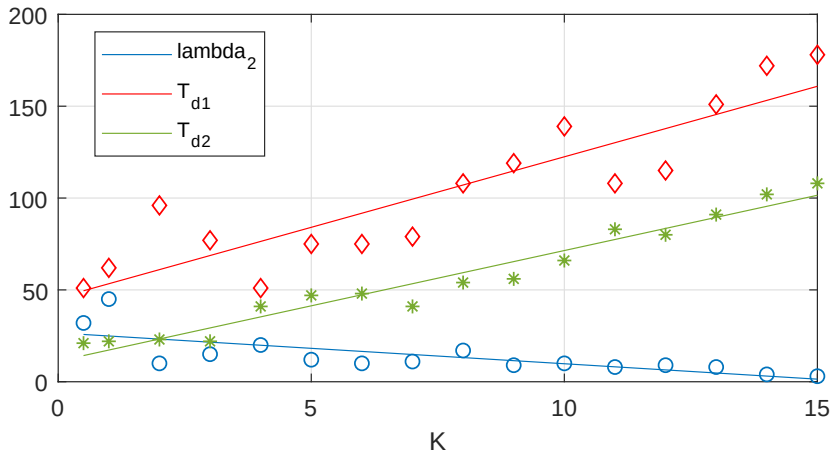

Figure 4.4: Interpolation of the λ_2, T_{d1} and T_{d2} parameters.

	Genetic Algorithms	**Interpolation**
IAE	5175	5182

Table 4.3: Average of the maximum IAE calculated for each value of K reported in table 4.2.

4.2.2 Robustness

Before executing the simulations it is necessary to establish a value of the ratio to be used. The K block in figure 4.1 is a gain that handles the presence of two inputs and one output in the process. By taking into account that, during maintenance phase the clinical practice suggests typical constant drug infusions of 6 $[mg/kg/h]$ of propofol and 0.2 $[\mu g/kg/min]$ of remifentanil, which correspond respectively to 0.12 $[mg/s]$ and 0.23 $[\mu g/s]$ for an average patient's weight of 70 $[kg]$. Thus, the ratio between remifentanil and propofol recommended rates, in the model units, is about 2 and the gain has been fixed to this value in order to test the most used configuration of the controller. In order to test the intra-patient robustness of the proposed control system a Monte Carlo method has been employed to verify the robustness property. In particular, a set of 1000 models have been generated for each patient of the database based on the statistical properties of the model parameters. The simulation results related to the average patient 13 for the induction phase are plotted in figure 4.5 and the corresponding performance indices are

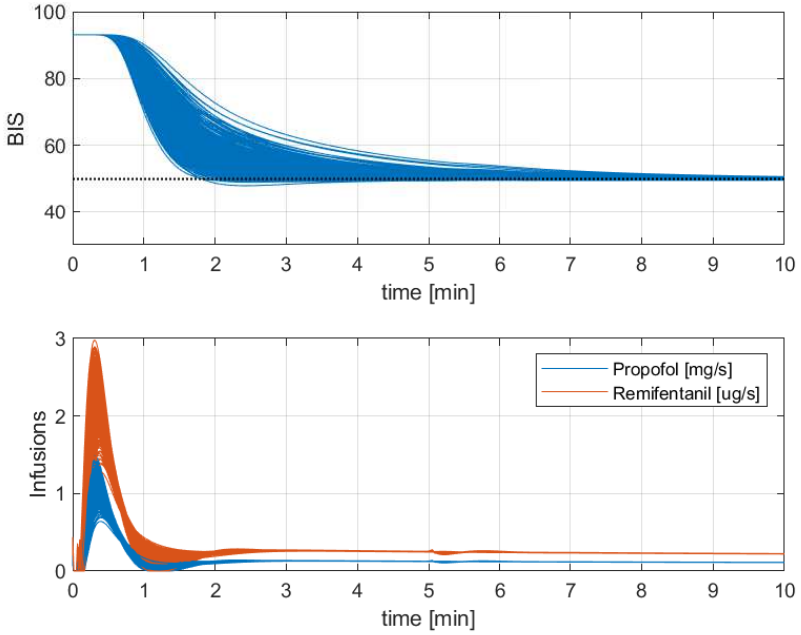

Figure 4.5: Monte Carlo simulation results of induction phase for the average patient 13.

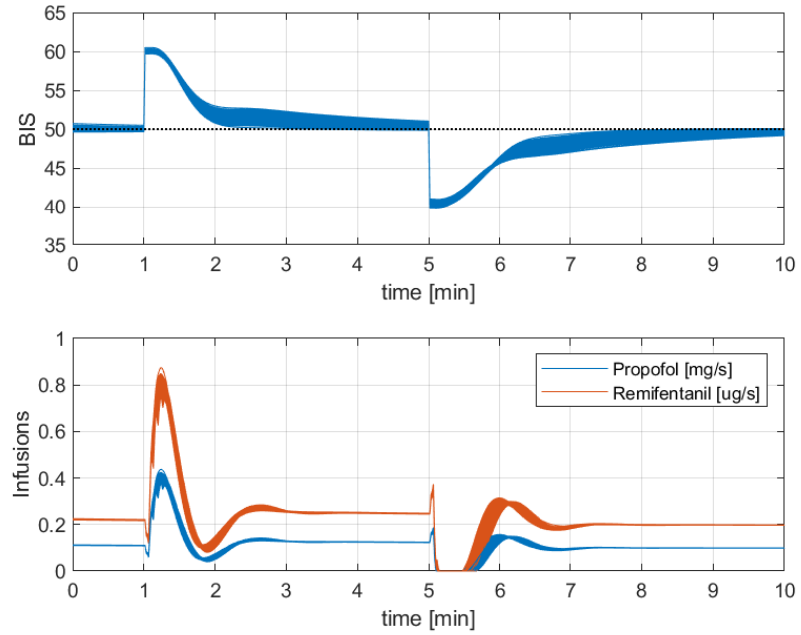

Figure 4.6: Monte Carlo simulation results of maintenance phase for the average patient 13.

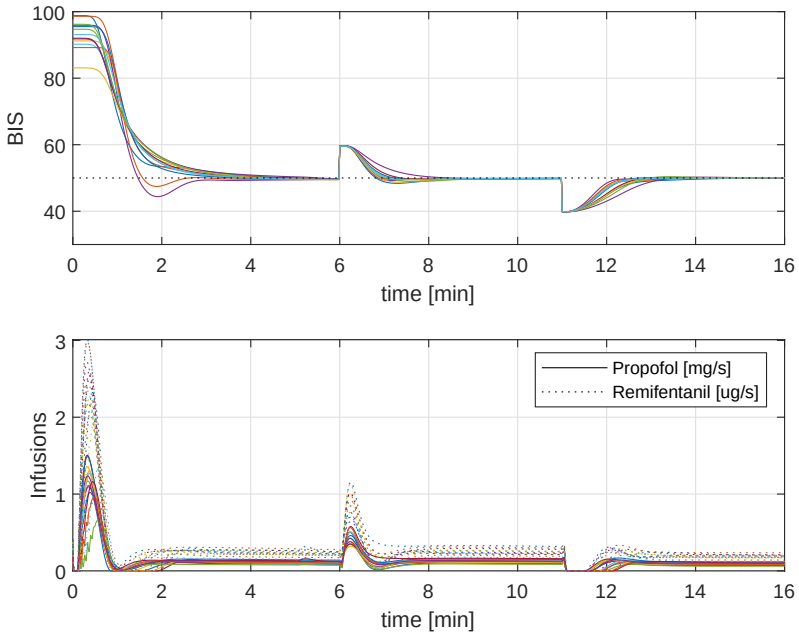

Figure 4.7: Simulation results of induction and maintenance phases for all patients.

	TT [min]	BIS-NADIR	ST20 [min]	ST10 [min]	US
mean	2.31	49.87	1.74	2.29	0.00
std.dev	0.51	0.15	0.29	0.51	0.00
min	1.40	47.99	1.22	1.38	0.00
max	5.25	50.71	3.60	5.23	0.00

Table 4.4: Performance indices for the induction phase with the MCM (average patient 13).

shown in table 4.4. Results for the maintenance phase are in figure 4.6 and in table 4.5. In both cases the results can be considered acceptable if we consider that in one case over 1000 the TT index is over the limit and that for this test we assume a significant variability of the system.

Regarding the inter-patient variability the results related to the induction and maintenance phases of all the patients of table 1.2 are shown in figure 4.7 and the performance indexes are reported in the next section. The achieved BIS level and the control actions are quite similar for each patient, and all the clinical specifications are always fulfilled, demonstrating the robustness of the system even with inter-patient variability.

	TTp [min]	BIS-NADIRp	TTn [min]	BIS-NADIRn
mean	0.61	49.93	0.88	50.14
std.dev	0.01	0.07	0.01	0.13
min	0.57	49.62	0.83	49.91
max	0.68	50.49	0.92	51.03

Table 4.5: Performance indices for the maintenance phase with the MCM (average patient 13).

4.3 Comparison with event based control

The MISO system developed for the combined propofol and remifentanil infusion has provided satisfactory results for automatic anesthesia control; in this paragraph we want to compare the developed control system with the one described in [39]. It is based on the implementation of an event generator with strong noise filtering capabilities together with a PIDPlus controller and considers both the administration of propofol and remifentanil in order to obtained a desired level of the BIS.

The control structure is shown in figure 4.8, where $r(t)$ is the set-point signal, $e(t)$ is the error variable and $up(t)$ $[mg/s]$ and $ur(t)$ $[\mu g/s]$ are the propofol and the remifentanil infusion rates, respectively. The saturation blocks limit the control signal with the same constraints introduced in table 4.1 and the ratio is set at 2.
In the paper the same performance indexes introduced in chapter 3 are used:

- TT: observed time-to-target (in seconds) required for reaching the first time the target interval of $[45 \div 55]$ BIS values;
- BIS-NADIR: the lowest observed BIS value;
- ST10: settling time, defined as the time interval for the BIS to reach and steady within the BIS range between 45 and 55 (that is, the target value of 50 ± 5);
- ST20: the same of ST10 but it considers a BIS range of 40 and 60;
- US: undershoot, defined as the difference between the lower threshold of 45 and the minimum value of BIS below this threshold.

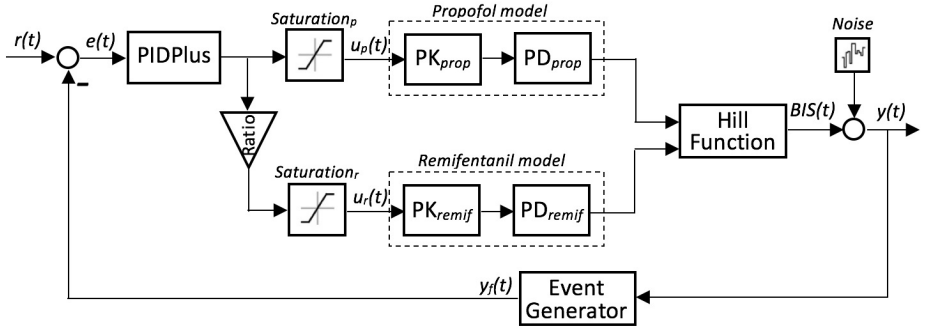

Figure 4.8: Control scheme used in [39]

	PIDPlus					GPC				
Patient	**TT [min]**	**BIS-NADIR**	**ST20 [min]**	**ST10 [min]**	**US**	**TT [min]**	**BIS-NADIR**	**ST20 [min]**	**ST10 [min]**	**US**
1	2.23	49.03	1.97	2.23	0.00	1.57	49.69	1.27	1.57	0.00
2	2.53	44.01	2.28	5.03	1.00	1.73	49.62	1.42	1.73	0.00
3	2.63	47.89	2.35	2.61	0.00	2.02	49.66	1.50	2.02	0.00
4	2.33	45.34	2.22	2.33	0.00	1.33	44.39	1.23	2.10	0.61
5	5.32	50.83	2.33	7.43	0.00	2.12	49.71	1.52	2.12	0.00
6	2.63	47.83	2.40	6.07	0.00	1.90	49.55	1.48	1.90	0.00
7	3.15	48.48	2.68	3.15	0.00	1.98	49.73	1.52	1.98	0.00
8	2.77	46.24	2.58	2.77	0.00	1.72	49.60	1.43	1.72	0.00
9	2.40	44.19	2.30	4.78	0.81	1.40	47.45	1.28	1.40	0.00
10	3.22	46.8	2.98	3.22	0.00	2.20	49.56	1.60	2.20	0.00
11	3.88	50.00	2.80	3.88	0.00	2.18	49.78	1.62	2.18	0.00
12	3.23	47.62	2.07	3.23	0.00	2.17	49.51	1.60	2.17	0.00
13	3.30	44.84	2.68	9.00	0.15	1.92	49.62	1.50	1.92	0.00
mean	3.05	47.16	2.43	4.29	0.15	1.86	49.07	1.46	1.92	0.05
std.dev	0.83	2.17	0.29	2.10	0.34	0.29	1.53	0.13	0.25	0.17
max	5.32	50.83	2.98	9.00	1.00	2.20	49.78	1.62	2.20	0.61
min	2.23	44.01	1.97	2.23	0.00	1.33	44.39	1.23	1.40	0.00

Table 4.6: Performance indices of induction phase for all patients.

	PIDPlus				GPC			
	TTp [min]	**BIS-NADIRp**	**TTn [min]**	**BIS-NADIRn**	**TTp [min]**	**BIS-NADIRp**	**TTn [min]**	**BIS-NADIRn**
1	1.30	48.39	1.53	50.50	0.45	48.66	1.05	50.08
2	0.92	47.45	1.30	52.06	0.48	49.63	0.80	50.08
3	0.95	47.13	0.93	51.58	0.48	49.72	0.78	50.09
4	0.88	46.33	0.97	53.17	0.48	49.29	0.72	50.01
5	1.33	50.00	1.96	51.32	0.55	49.65	1.02	50.09
6	1.32	46.61	1.28	52.34	0.52	49.62	0.83	50.06
7	1.70	49.20	1.81	52.43	0.58	49.77	1.00	50.05
8	1.55	48.73	1.32	50.57	0.53	49.69	0.87	50.03
9	1.07	45.85	0.93	53.31	0.48	49.60	0.78	50.04
10	1.00	46.84	0.95	54.62	0.48	49.05	1.05	50.08
11	2.56	50.00	2.58	50.55	0.73	49.85	1.32	50.06
12	1.72	49.81	1.60	50.43	0.53	49.27	1.13	50.27
13	1.10	48.08	1.05	52.75	0.53	49.69	0.85	50.06
mean	1.34	48.03	1.40	51.97	0.53	49.50	0.94	50.08
std.dev	0.47	1.45	0.49	1.30	0.07	0.34	0.17	0.06
max	2.56	50.00	2.58	54.62	0.73	49.85	1.32	50.27
min	0.88	45.85	0.93	50.43	0.45	48.66	0.72	50.01

Table 4.7: Performance indices of maintenance phase for all patients.

In tables 4.6 and 4.7 are reported the performance indices obtained with the two controllers for the induction and maintenance phases. As it is possible to see from the TT and ST indices, with the GPC developed in this work it is possible to obtain faster set-point responses with an average lower undershoot. Also during the maintenance phase the GPC presents a faster reaction, having TTp and TTn smaller than the PIDPlus. The main reason of these differences is attributable at the internal presence of the model into the controller, necessary for estimating the future system response in advance, it allows the GPC to modify the control action accordingly, reaching the reference optimally.

Regarding the robustness, the most critical aspect for every model based controller, the same test performed in [39] have been reproduced. The results, reported in tables 4.8 and 4.9, show that GPC meet the specifications even with uncertainties in the linear part, obtaining good performance indexes.
It can therefore be concluded that the predictive control system developed is preferable to the event based control for the particular type of application considered.

	PIDPlus					GPC				
Patient	**TT [min]**	**BIS-NADIR**	**ST20 [min]**	**ST10 [min]**	**US**	**TT [min]**	**BIS-NADIR**	**ST20 [min]**	**ST10 [min]**	**US**
mean	3.38	47.74	2.85	4.22	0.13	2.31	49.87	1.74	2.31	0.00
std.dev	0.94	1.91	0.87	1.72	0.62	0.51	0.15	0.29	0.51	0.00
min	2.47	39.79	2.23	2.47	0.00	1.40	47.99	1.22	1.38	0.00
max	5.98	51.41	9.27	9.98	5.20	5.25	50.71	3.60	5.23	0.00

Table 4.8: Performance indices for the induction phase with the MCM (average patient 13).

	PIDPlus				GPC			
	TTp [min]	**BIS-NADIRp**	**TTn [min]**	**BIS-NADIRn**	**TTp [min]**	**BIS-NADIRp**	**TTn [min]**	**BIS-NADIRn**
mean	1.28	48.30	1.37	48.30	0.61	49.93	0.88	50.14
std.dev	0.18	0.66	0.21	0.67	0.01	0.07	0.01	0.13
max	2.56	46.15	0.97	46.15	0.57	49.62	0.83	49.91
min	1.78	49.41	2.12	49.42	0.68	50.49	0.92	51.03

Table 4.9: Performance indices of maintenance phase with the MCM (average patient 13).

Conclusions and future works

In this work an automatic control system for intravenous anesthesia was developed. The system exploits the estimated effect-site concentration, derived from the BIS signal, as an anesthetic level feedback for the regulation of propofol and remifentanil, hypnotic and anesthetic drugs respectively. The novelty of this work lies in the use of the GPC to anticipate the responses of the patients to drug infusion, and an innovation feedback signal to compensate for model uncertainties.

The control structure has been implemented initially for the propofol infusion only, leading to the study of a SISO model of the process. After appropriately calibrating the system with GA, system simulations with patient models in the literature were performed. The system meets all the medical specifications required on the BIS profile trend, representing a good starting point for the development of the complete control system.. We also compared the performance of the controller with other systems found in the literature, noting that the developed system presents many advantages.
As the results obtained with the SISO system are excellent, the control structure has been then expanded to consider the introduction of the remifentanil effect on the process. This represents a significant control challenge, as the response of the human body to the infusion of propofol and remifentanil can be modeled through a non-linear MISO system that must take into account the synergistic effect of drugs. For the regulation of propofol, the same GPC controller developed for the SISO system was maintained. The lack of feedback signals to detect the sensation of pain does not allow the realization of a closed control loop also for remifentanil. It was therefore decided to regulate the anesthetic as a ratio over the

hypnotic drug, as done in the clinical practice. In this case, the medical specifications are also met and the controller reacts well to disturbances and changes in the set-point.

One of the most interesting control challenges of this system is undoubtedly robustness, as the GPC controller is very sensitive to model changes. In fact there is a great variability of the process, depending on the patient considered. Each person reacts differently to the administration of drugs, depending on their physical characteristics and health condition. The system must therefore compensate for intra-patient variability, always guaranteeing excellent infusion profiles not harmful to the patient's health. For this reason we placed emphasis on testing the robustness for intra-patient and inter-patient variability with a MCM.

In future works it will be interesting to improve the control of the remifentanil by looking for a method to make a closed loop. It is not to be excluded that future works could integrate in the automatic control also the neuromuscular blocking drugs not considered yet. As an ultimate ambitious goal, there is obviously the implementation of the controller and the execution of tests on real patients.

The implementation of a closed-loop control system could lead to advantages for the health of patients and economic benefits at the same time. The maintenance of the hypnotic level around a recommended BIS value could allow a reduction of the time required for the awakening of the patient, and consequently it could lead to a save of time for the medical staff. The work of the anesthesiologist could be facilitated, allowing a reduction in workload. Moreover, the patient would benefit from limited postoperative side-effects following the propofol infusion and would require less time for the anesthesia and psychomotor function recovery. It is therefore believed that it is of paramount importance to continue with the development of this system by achieving a functioning control scheme that respects the medical specifications and is robust in terms of inter and intra-patient variability.

Bibliography

[1] T. Mendonça, J.M. Lemos, H. Magalhães, P. Rocha, and S. Esteves. Drug delivery for neuromuscular blockade with supervised multimodel adaptive control. *IEEE Transactions on Control System Technology*, 17(6):1237–1244, 2009.

[2] A. Krieger and E.N. Pistikopoulos. Model predictive control of anesthesia under uncertainty. *Computers & Chemical Engineering*, 71:699 – 707, 2014.

[3] L. Merigo, M. Beschi, F. Padula, N. Latronico, M. Paltenghi, and A. Visioli. Event based control of propofol and remifentanil coadministration during clinical anesthesia. In *2017 3rd International Conference on Event-Based Control, Communication and Signal Processing (EBCCSP)*, pages 1–8, May 2017.

[4] S. Bibian. *Automation in clinical anesthesia*. Master Thesis, Vancouver, Canada, 1999.

[5] T. Newman. What's to know about general anesthesia? *Medical News Today. MediLexicon*, 5 Jan. 2018.

[6] C. Prys-Roberts. Anaesthesia: a practical or impractical construct? *British Journal of Anaesthesia*, 59(11):1341 – 1345, 1987.

[7] J.S. Shieh, D.A. Linkens, and J.E. Peacock. Hierarchical rule-based and self-organising fuzzy logic control for depth of anaesthesia. *IEEE Trans Syst Man Cybern Part-C*, 29:98–109, 1999.

[8] P. Olivier, D. Sirieix, P. Dassie, N. D'Attelis, and J. Baron. Continuous infusion of remifentanil and target-controlled infusion of propofol for patients undergoing cardiac surgery: a new approach for scheduler early extubation. *Cardiothorac Vasc Anesth*, 14:29–35, 2000.

[9] A. Viby and J. Mogensen. *Neuromuscular Monitoring*. Miller's Anesthesia 7th Edition, Churchill Livingstone, 2009.

[10] A.L. Vanluchene, H. Vereecke, O. Thas, E.P. Mortier, S.L. Shafer, and M.M. Struys. Spectral entropy as an electroencephalographic measure of anesthetic drug effect: a comparison with bispectral index and processed midlatency auditory evoked response. *Anesthesiology*, 101:34–42, 2004.

[11] D. Copot and C. M. Ionescu. Drug delivery system for general anesthesia: Where are we? In *2014 IEEE International Conference on Systems, Man, and Cybernetics (SMC)*, pages 2452–2457, Oct 2014.

[12] K. van Heusden, J. M. Ansermino, and G. A. Dumont. Robust miso control of propofol-remifentanil anesthesia guided by the neurosense monitor. *IEEE Transactions on Control Systems Technology*, PP(99):1–13, 2017.

[13] G.A. Dumont, A. Martinez, and J.M. Ansermino. Robust control of depth of anesthesia. *International Journal of Adaptive Control and Signal Processing*, 23:435–454, 2009.

[14] J.B. Glen. The development of diprifusor: a tci system for propofol. *Anaesthesia*, 53:13–21, 1998.

[15] P. Wen A. Shahab. Depth of anesthesia control using internal model control techniques. In *IEEE/ICME International Conference on Complex Medical Engineering (CME)*, 2010.

[16] C.M. Ionescu, R. De Keyser, B.C. Torrico, T De Smet, M.M. Struys, and J.E. Normey-Rico. Robust predictive control strategy applied for propofol dosing using BIS as a controlled variable during anesthesia. *IEEE Transactions on Biomedical Engineering*, 55(9):2161–2170, 2008.

[17] M.M. Silva, T. Mendonça, and T. Wigren. Online nonlinear identification of the effect of drugs in anaesthesia using a minimal parameterization and BIS measurements. In *American Control Conference*, Marriott Waterfront, Baltimore, MD, USA, 2010.

[18] F. Padula, C. Ionescu, N. Latronico, M. Paltenghi, A. Visioli, and G. Vivacqua. Inversion-based propofol dosing for intravenous induction of hypnosis. *Communications in nonlinear science and numerical simulation*, 39:481–494, 2016.

[19] H. Araujo, B. Xiao, C. Liu, Y. Zhao, and H. Lam. Design of type-1 and interval type-2 fuzzy pid control for anesthesia using genetic algorithms. *Journal of Intelligent Learning Systems and Applications, 6*, pages 70–93, 2014.

[20] F.N. Nogueira, T. Mendonça, and P. Rocha. Controlling the depth of anesthesia by a novel positive control strategy. *Computer Methods and Programs in Biomedicine*, 114(3):e87 – e97, 2014.

[21] T.W Schnider, C.F Minto, P.L. Gambus, C. Andresen, D.B. Goodale, S.L. Shafer, and E.J. Youngs. The influence of methon of administration and covariates on the pharmacokinetics of propofol in adult volunteers. *Anesthesiology*, 88:1170–1182, May 1998.

[22] C.F. Minto, T.W. Schnider, T.D. Egan, E. Youngs, H.J. Lemmens, P.L. Gambus, V. Billard, J.F. Hoke, K.H. Moore, D.J. Hermann, and K.T. Muir. Influence of age and gender on the pharmacokinetics and pharmacodynamics of remifentanil. *Anesthesiology*, 86:10–23, 1997.

[23] B. Andrade Costa, M. Silva, T. Mendonça, and J.M. Lemos. Neuromuscular blockade nonlinear model identification. In *17th Mediterranean Conference on Control & Automation*, Tessalonica, Grecia, 2009.

[24] M.M. Silva, T. Wigren, and T. Mendonça. Nonlinear identification of a minimal neuromuscular blockade model in anaesthesia. *IEEE Transactions on Control System Technology*, 20(1):181–188, 2011.

[25] T. Buillon, J. Bruhn, L. Radulescu, C. Andersen, S. Park, and T. Shafer. Pharmacodynamic interaction between propofol and remifentanil regarding hypnosis, tolerance of laryngoscopy, bispectral index and electroencephalographic approximate entropy. *Anesthesiology*, 100(6):1353–1372, 2004.

[26] T. Buillon, J. Bruhn, L. Radulescu, E. Bertaccini, S. Park, and T. Shafer. Non-steady state analysis of the pharmacokinetic interaction between propofol and remifentanil. *Anesthesiology*, 97(6):1350–1362, 2002.

[27] C.F. Minto, T.W. Schnider, T.G. Short, K.M. Gregg, A. Gentilini, and S.L. Shafer. Response surface model for anesthetic drug interactions. *Anesthesiology*, 92(6):1603–1616, 2000.

[28] T. Koitabashi, J.W. Johansen, and P.S. Sebel. Remifentanil dose/electroencephalogram bispectral response during combined propofol/regional anestesia. *Anesthesia & Analgesia*, 94(6):1530–1533, 2002.

[29] S.E. Kern, G. Xie, J.L. White, and T.D. Egen. A response surface analysis of propofol-remifentanil pharmacodynamic interaction in volunteers. *Anesthesiology*, 100(6):1373–1381, 2004.

[30] D.W. Clarke, C. Mohtadi, and P.S. Tuffs. Generalized predictive control - part i. the basic algorithm. *Automatica*, 23(2):137 – 148, 1987.

[31] D.W. Clarke, C. Mohtadi, and P.S. Tuffs. Generalized predictive control - part ii extensions and interpretations. *Automatica*, 23(2):149 – 160, 1987.

[32] D.W. Clarke. Application of generalized predictive control. *IFAC Proceedings Volumes*, 21(7):1 – 8, 1988. 2nd International IFAC Symposium on Adaptive Control of Chemical Processes 1988 (ADCHEM '88), Lyngby, Copenhagen, Denmark, 17-19 August.

[33] E.F. Camacho and C. Bordons. *Model Predictive Control*. Springer-Verlag, London, 2007.

[34] D.P. Kroese, T. Brereton, T. Taimre, and Z.I. Botev. Why the monte carlo method is so important today. *Wiley Interdisciplinary Reviews: Computational Statistics*, 6(6):386–392, 2014.

[35] C.Z. Mooney and M.C. Z. *Monte Carlo Simulation*. Number No. 116 in Monte Carlo Simulation. Sage Publications, inc, 1997.

[36] R.Y. Rubinstein. *Simulation and the Monte Carlo Method*. John Wiley & Sons, Inc., New York, NY, USA, 1st edition, 1981.

[37] E. J. McGrath, S. L. Basin, R. W. Barton, D. C. Irving, S. C. Jaquette, W. R. Ketler, and C. A. Smith. *Techniques for efficient Monte Carlo simulation*. Science Applications, Inc., 1250 Prospect Street La Jolla, California 92037, 1973.

[38] L. Merigo, F. Padula, A. Pawlowski, S. Dormido, J. Guzmán, N. Latronico, M. Paltenghi, and A. Visioli. A model-based control scheme for depth of hypnosis in anesthesia. *Biomedical Signal Processing and Control*, 42, 04 2018.

[39] A. Pawlowski, L. Merigo, J.L. Guzmán, S. Dormido, and A. Visioli. Two-degree-of-freedom control scheme for depth of hypnosis in anesthesia. *IFAC-PapersOnLine*, 51(4):72 – 77, 2018. 3rd IFAC Conference on Advances in Proportional-Integral-Derivative Control PID 2018.

[40] L. Merigo. *Studio di un Sistema di Controllo per Anestesia Endovenosa*. Master thesis at Università degli studi di Brescia, Brescia (IT), 2015.